2009

Efficiency of Cellulase Enzyme Immobilized on Magnetic Nanoparticles

Jason Jordan
Louisiana State University and Agricultural and Mechanical College

EFFICIENCY OF CELLULASE ENZYME IMMOBILIZED ON MAGNETIC NANOPARTICLES

A Thesis

Submitted to the Graduate Faculty of the
Louisiana State University and
Agricultural and Mechanical College
in partial fulfillment of the
requirements for the degree of
Master of Science in
Biological and Agricultural Engineering

in

The Department of Biological and Agricultural Engineering

by
Jason Jordan
B.S., Louisiana State University, 2006
August 2009

ACKNOWLEDGMENTS

I would like to thank the Department of Biological and Agricultural Engineering at Louisiana State University and the LSU AgCenter for funding this research. I would also like to thank my major professor, Dr. Chandra Theegala, for his guidance and sharing his wealth of knowledge and experience in helping further my education.

Special thanks go to Dr. Challa Kumar for his help both as a committee member and for sharing his time and knowledge pertaining to nano-particle research. Thanks also to Dr. Donal Day for his involvement in the committee for this thesis.

Very special thanks to Chang-Ho Chung of the Audubon Sugar Institute for his help in understanding the nature of the cellulase enzyme and the hydrolysis of cellulosic materials. Thanks also to the following people for their support and patience in helping conduct my analysis: Cindy Henk, Lee Madsen, Balaji Gopolan, Raphael Cueto and Dongmei Cao.

Finally, thanks to all my family and friends for their unwavering support and to my student workers, Corey Rohrbach and Colton Adkins, without whom this research would not have been possible.

TABLE OF CONTENTS

LIST OF TABLES

LIST OF FIGURES

ABSTRACT

Advances in enzymatic hydrolysis have developed new methods for conversion of lignocellulosic biomass into fermentable sugars for various applications, mainly ethanol production. The present study involves immobilization of a cellulase enzyme complex on a solid support which can be recovered for subsequent use in multiple reactions. The supports of interest include Fe_3O_4 nanoparticles (~13 nm) and polystyrene-coated particles containing a Fe_3O_4 core (1-2 μm). Each support contains amine functional groups based on the surface that allow covalent attachment of enzymes via carbodiimide activation. The nanoparticles were characterized using transmission electron microscopy (TEM) and immobilization was confirmed using Fourier transform infrared (FTIR) spectroscopy and X-ray photoelectron spectroscopy (XPS). The nanoparticles were successfully recycled 6 times and the polystyrene-coated microparticles 4 times before their corresponding activity levels had fallen below 10%. Activity was determined using a dinitrosalicylic acid (DNS) assay, which detected the total reducing sugars present. Sugar production was confirmed by high performance liquid chromatography (HPLC) with the highest concentration of sugars detected as glucose with minimal amounts of xylose and cellobiose also present. Activity retention was 30.2% of the free enzymes activity following immobilization on the magnetite nanoparticles and 26.5% after immobilization on the polystyrene-coated particles. A performance evaluation over all recycles indicated that 78% of the free enzyme sugars were produced by magnetite nanoparticles and 42% produced by polystyrene-coated particles following 96 hours of hydrolysis. Further characterization of the magnetite nanoparticles revealed that maximum protein attachment (~90%) occurred at low enzyme loadings (1-2 mg). The enzyme-to-support saturation point occurred at a weight ratio of 0.02. Thermal measurements for the nanoparticles indicated increased stability over a broader

range of temperatures with a peak temperature of 50˚C. Ionic forces between the enzyme and support surface caused a shift in pH from 4.0 to 5.0, and stability was assessed over 72 hours of hydrolysis with the free enzyme losing 49% $\pm$ 0.05% of its activity while the activity of the immobilized enzyme complex had dropped by only 42% $\pm$ 0.53%. An activity comparison was assessed to compare the performance of Fe_3O_4 nanoparticles and polymeric microparticles, noting the advantages and disadvantages of each.

1 INTRODUCTION

1.1 Ethanol as an Alternative Fuel

Due to the increasing demand for energy, newer fuels are repeatedly being brought into the limelight to combat this global situation. One of particular interest is ethanol. Since the nineteenth century, ethanol has been known for its combustion properties to produce heat energy. The chemical structure of ethanol contains a hydroxyl group and a short hydrocarbon chain. This structure allows for increased hydrogen bonding rendering it more viscous and less volatile than less polar compounds of similar molecular weight.

Petroleum products are the chief form of energy used today and have been for the past 150 years. Easy accessibility and little need for refining make it the most proficient fuel source available. In recent years, however, the abundant use of petroleum has proven to be detrimental to both the economy and the environment. Depleted oil reserves have forced the onset of offshore drilling which has been consistently moving further out to sea. This further exploration raises the barrel price of oil and limited reserves in the United States are forcing the import of foreign oil to meet the nation's energy demands. In addition to economic burdens, the burning of petroleum products has demonstrated evidence of harmful byproducts being released into the earth's atmosphere. Many scientists believe that this process has accelerated a rise in atmospheric temperatures, which has frequently been dubbed as global warming.

1.2 Comprehensive Overview

Currently, the production of ethanol relies mainly on the use of simple carbohydrates produced by various agricultural supplies which include corn and sugarcane. Limited availability and the cost of removing these products from a food source allow a minimum amount of ethanol to be produced within the US as compared to the overall demand for energy.

Due to these complications, cellulose is considered to be a viable alternative. Total biomass production in the US is estimated to be approximately 2.8 billion tons annually, which has the potential for 5.14 x 10^7 MJ of energy per year (assuming 17.6 MJ per kg of biomass[1]). Currently, biomass supplies over 3% of the total energy consumption in the United States with a projected increase of 2% annually through 2030[2].

Cellulose is the most abundant biopolymer on earth. Found in virtually all plant cell wall matter, it has an almost limitless supply. Often found as part of the biomass complex in combination with hemicelluloses and lignin, it gives strength to the cell wall and structure and stability to the plant. Of key interest to cellulosic biomass is its hydrophobicity. Cellulose crystalline structures make it completely water-insoluble. Its close association with lignin further increases its impermeability to water. Typically, certain pretreatment methods are employed to reduce its hydrophobicity and create an easier approach for penetration of the cellulose structure.

Currently, there are three main methods for breaking down cellulose into simple sugars for eventual ethanol production; these are acid hydrolysis, enzymatic hydrolysis, and thermo-chemical conversion. Acid processes are the oldest methods and are sometimes conducted under high temperatures and pressures. Sugar recovery efficiency is usually 50-90%, and it can sometimes produce some unwanted byproducts[3]. One byproduct in particular is furfural (a chemical used in the plastics industry) which can be poisonous to the fermentation microorganisms. An enzymatic process uses naturally occurring proteins to break down large cellulose chains. This method is highly efficient and is achieved under relatively mild conditions, but can be quite expensive[3]. Finally, thermo-chemical processes involve gasification of cellulosic biomass to produce a synthesis gas which can later be converted to

ethanol. Ethanol yields up to 50% have been obtained using this method; however, a cost-effective process has yet to be produced[3]. Enzymatic processes tend to be favorable due to their specificity and amiable operating conditions.

Enzymes are defined as biomolecules which catalyze chemical reactions. They are almost always proteins and each has specific functions. The cellulase enzyme complex refers to a class of enzymes produced mainly from a variety of fungi, such as *Trichoderma reesei*, *Trichoderma viride*, and *Apergillus niger*, etc., as well as some bacteria. They each work in a synergistic manner for hydrolyzing cellulose to beta-glucose. A schematic outlining this conversion is displayed in Figure 1.1.

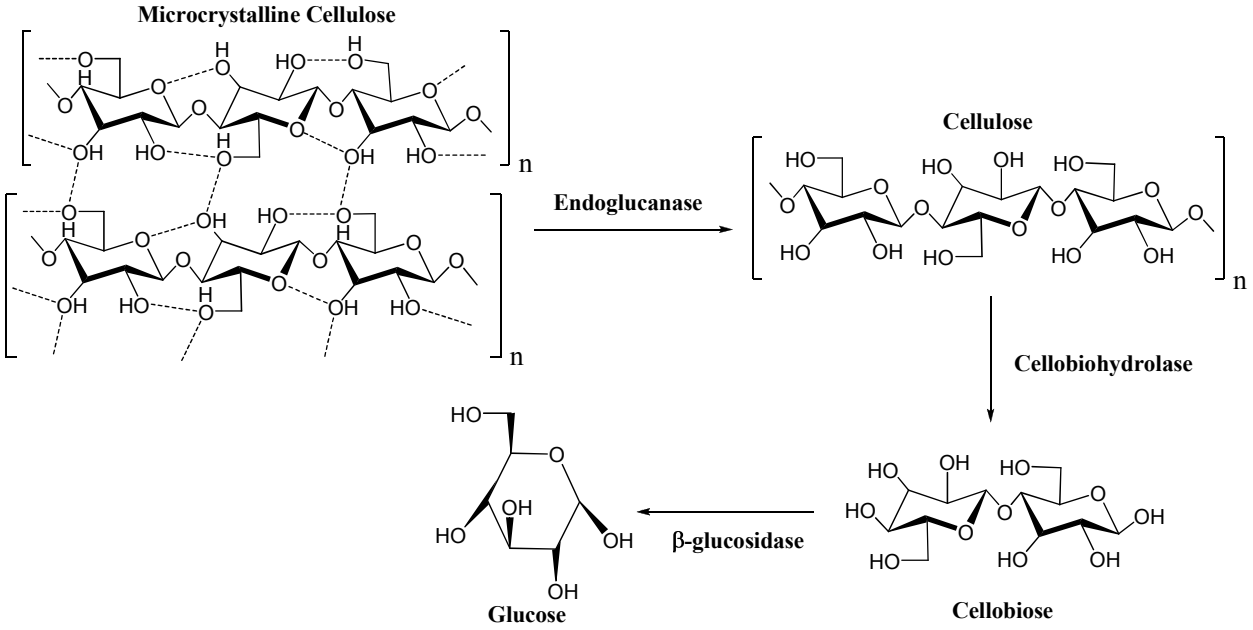

Figure 1.1: Cellulase enzyme complex hydrolyzing microcrystalline cellulose to individual glucose monomers.

Enzymes, in contrast to the biomass complex, are hydrophilic in nature. Their water-permeable structure only permits single usage when reacting in solution; this, in turn, results in higher prices for ethanol production. To combat this situation, ongoing research has opted

toward immobilization on to a solid support making the water-soluble enzyme restricted in movement and more accessible for recovery. Supports often administered include entrapment within gel matrices, encapsulating in a membrane shell, surface absorption, covalent bonding to a solid support, among other well-known variations[4]. With regards to the complete cellulase system, concern must be noted to permit total attachment of the enzyme complex in order to continue working in its synergistic manner and contributing complete hydrolysis of cellulose to an individual glucose monomer form.

The enzyme, as part of the enzyme-substrate complex, must be applied in a free form to permit its active sites to come in contact with substrate. In the case of the cellulase-cellulose complex, cellulose is much larger in size as compared to the enzyme. A problem thus ensues when using certain immobilization methods, such as entrapment within a gel matrix, as the active sites on the enzyme would become unreachable by the substrate. A more acceptable possibility is encountered by covalently bonding the enzyme to a solid support. Although certain sites of the cellulase molecule are rendered inactive due to binding with the support, and possibly lowering its activity, the majority of the molecule remains open allowing for direct contact with the biomass substrate. Covalent binding may also become more efficient, as compared to the free enzyme form, during the hydraulic reaction due to a relatively short distance between the associated enzymes in the cellulase complex, allowing for reaction products to become more readily available to subsequent components at higher concentrations[4]. In nature, many sequential enzymatic reactions occur in tight aggregates, in gel-like encapsulation, or embedded in a shell membrane[5]. Size and material are also important factors, as a heavier support may reduce mobility of the enzyme in solution and prevent complete contact with substrate, and the material selection would determine the method of extraction. With these factors considered, the

ensuing research focused on the use of cellulase enzyme immobilized on superparamagnetic iron oxide nanoparticles (SPION). The nature of nano-sized particles, due to their extremely small size, allows for equal dispersion and longer suspension time within a solution. The magnetic properties of iron oxide (magnetite) warrant secure immobilization for extraction of surrounding solution. The overall goal of this study was to evaluate a method for immobilization of the cellulase enzyme complex that would improve its recovery efficiency while retaining reasonable enzyme activity.

1.3 Research Objectives

The objectives of the proposed research include, but are not limited to:

1. Immobilization of cellulase enzyme onto co-precipitated iron oxide nanoparticles and establishing a baseline activity.
2. Immobilization of cellulase enzyme on polystyrene-coated iron oxide particles with comparison to Objective 1.
3. Recovery of immobilized cellulase enzymes for use in multiple hydrolysis reactions and evaluation of enzyme activity after repeated use.
4. Characterization of enzyme-bound nanoparticles to determine optimum operating parameters which will allow for maximum efficiency.

1.4 A Note on Activity Units

According to Ghose (1987), through the nature of most cellulase work, investigators in various laboratories have each developed a series of empirical assay procedures which have resulted in a situation where comparison of cellulase activities is not relatively made in a quantitative manner[6]. Some commonly used activity assay methods include Filter Paper Assay

(FPU), Cellobiase Assay, and Carboxymethyl Cellulase Assay, among others. Due to the properties of the cellulase enzyme complex, enzyme preparations should be compared on the basis of significant and equal conversion. For example, twice as much enzyme will give equal sugar in half the time, but it will not give twice as much sugar in equal time. With the employment of low levels enzyme used in this study, it will not be practical to implement any of the preceding assay methods for the ensuing research. Therefore, the amount of glucose produced through enzymatic hydrolysis of cellulosic biomass will be calculated and activity measurements throughout this thesis will be further addressed using the units of [(μmol of glucose produced)/ (mg enzyme)-hr].

2 LITERATURE REVIEW

2.1 Cellulosic Biomass Complex

Established knowledge says cellulosic fibers display a physical structure consisting of long, unbranched polymer chains of anhydroglucose monomer units linked by β-1,4-glycosidic bonds. These chains are known to consist of over 10,000 glucose residues[7]. When comparing cellulosic morphology to starch polymers found typically in cereal grains, the structures are not dissimilar. The only difference pertains to a α-1,4-glycosidic bond in the starch molecule instead of the β-1,4-bond found in cellulose. This morphology gives starch a curved, and sometimes branched, structure allowing relatively easy access for enzymatic penetration to produce a more efficient endpoint of hydrolysis to glucose monomers. The cellulosic structure portrays microfibrils containing long, unbranched chains ordered in a highly crystalline form which are practically impenetrable, even to water molecules. The structure of native cellulose is shown in Figure 2.1. During cellulose biosynthesis, individual glucan chains adhere to each other by hydrogen bonding and van der Waals forces to crystallize and form insoluble networks[7].

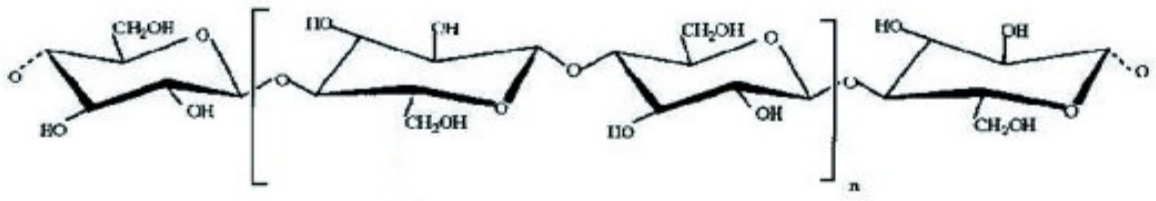

Figure 2.1: Structural formula of cellulose with individual cellobiose molecule enclosed in brackets[7].

Upon observation of plant cell wall structures, cellulose occurs mostly as lignocelluloses in complex association with lignin, as well as hemicelluloses[8]. Distinctive characteristics of lignocelluloses make them resistant to attack by outside biological forces and, therefore,

providing a structure that is particularly complex and heterogeneous[9]. Nevertheless, through ongoing research, the challenges of converting cellulose into a usable form are becoming a more achievable prospect by employment of well-known procedures for destructing the long polymer chains into individual glucose monomers. The stated procedures may consist of acid hydrolysis, thermo-chemical conversion, or enzymatic hydrolysis which normally involves the reaction of a water molecule with each glucose molecule produced[3]. The use of enzymatic compounds is of particular interest and, therefore, will be employed in the ensuing research.

Upon observation of the biomass complex, it should be noted that the close association of cellulose with lignin would affect the absorption and hydrolysis efficiencies of cellulase enzymes. Cellulases have been shown to readily adsorb to both isolated lignin,[10] and lignaceous residues remaining after complete hydrolysis of the cellulose component[11, 12]. The presence of lignin decreases hydrolysis by preventing complete adsorption of enzymes on to cellulosic substrate. Therefore, lignocellulosic biomass must be structurally modified into a pure form of cellulose in order to achieve maximum hydrolytic conversion. Biomass pretreatments have proven to be an effective solution for improving biodegradation. Well known pretreatment methods include the use of dilute acid, steam explosion, alkaline wet oxidation, ultrasonication, and milling, to name a few[8, 13-17]. Several pretreatment methods have been demonstrated to be effective in disrupting the lignin-carbohydrate complex,[11, 18] or the highly ordered cellulose structure itself[19]. Most success has occurred through employment of treatments involving a physical disruption of the structure itself.

2.2 Components and Properties of Cellulase Enzyme

Cellulase (EC 3.2.1.4) enzymes are found typically in various fungi, bacteria, and protozoans which catalyze the hydrolysis of cellulose found in decaying plant material. Well-

known species where cellulase can be found include *Trichoderma ressei*, *Trichoderma viride*, and *Aspergillus niger*, to name a few[20-22]. Cellulase, such as that found in *Trichoderma* species, is produced by subjecting the species to cellulosic substrate. It is produced when cellulose is present in the medium but not when substrates, such as glucose, are the sole carbon source, which is why cellulase is referred to as an inducible enzyme[4].

Cellulase itself is a complex, multi-component system containing mixtures of endoglucanases (EG), cellobiohydrolases (CBH), and β-glucosidase[23]. The generally accepted mechanism of cellulolytic hydrolysis is that endoglucanases, cellobiohydrolases, and β-glucosidases work in a synergistic manner[24, 25]. EG works to disrupt the microcrystalline structure of cellulose and expose individual polysaccharide chains[21]. CBH cleaves cellotrioses and cellobioses from the ends of the exposed chains produced by EG. There are two types of CBH, one which attacks the reducing end of the terminus chain and the other which attacks the non-reducing end. CBH does not typically attack microcrystalline cellulose, although, one produced from *Trichoderma reesei* has been shown to degrade highly crystalline and ordered cellulose without the help of any EG activity[26-28]. β-Glucosidases cleave the CBH product polymers into individual glucose monosaccharides, but have no effect on crystalline cellulose[4]. The extracellular β-glucosidase of *Trichoderma* species are generally present in low levels when the organism is cultured on cellulose because it is inactivated under the acid conditions which develop in the medium while the other enzymes of the cellulase complex are more stable[29]. The *Aspergilli* species (*A. niger* and *A. phoenicis*), however, are known to be superior producers of β-glucosidase[30]. It has been determined that when *Trichoderma* cellulase preparations are supplemented with β-glucosidase from *Aspergillus* during practical saccharifications, glucose is the predominant product and the rate of saccharification is significantly increased[30].

Of additional importance in the hydrolysis of cellulosic biomass is the use of the enzyme xylanase. Xylanase is useful in disrupting hemicellulose sugar chains found in various biomass substrates, of which xylose is a major component. The typical source for production is via the *Aspergillus* species. When dealing with the lignocellulosic complex, it has been shown that the addition of xylanase enriched product, with cellulase supplemented preparations, significantly enhanced the saccharification rate while increasing hydrolysis kinetics[31].

2.3 Enzymatic Saccharification of Cellulose

Hydrolysis of cellulosic biomass using an enzymatic approach involves merely introduction of the cellulase enzyme onto substrate at a specified temperature and pH level that is adequate to keep the enzyme stable. The basic method is best demonstrated by the laboratory analytical procedure (LAP-009) concocted by the National Renewable Energy Laboratory (NREL)[32]. Research behind this procedure has been effective in ascertaining the most efficient reaction possible, which includes correct enzyme loading, appropriate substrate-to-volume ratio, and sterility techniques, in addition to proper pH and temperature control for the type of enzyme used.

The concept of hydrolysis involves a chemical reaction in which a chemical compound is broken down by reacting with water. Equation 1[33] shows the stoichiometric reaction of cellulose with water to produce glucose (saccharification). Multiple studies include the use of different enzymes, various substrates, and alterations of environmental conditions for comparison purposes that will aide in the achievement of optimum hydrolysis. Peiris and Silva (1987) showed that different cellulases produced from *Trichoderma* strains produced comparable results when hydrolyzing rice straw[34]. Imai et al. (2004) combined multiple cellulases from *Trichoderma* and *Aspergillus* species for comparison and discovered that a mixed-enzyme

system gave improved hydrolytic activity over single-enzyme systems[8]. Herr (1980) demonstrated the effects of subjecting various substrates to a specific strain of *Trichoderma viride* which contains a higher concentration of β-glucosidase. In conjunction with a continuous removal of glucose, the high loading of β-glucosidase produced higher glucose yields when compared to other cellulase enzymes. This has proven important when considering the inhibition effects of glucose on β-glucosidase and cellobiose on EG and CBH[35]. This was also demonstrated in part by Sun and Cheng[36].

$$[C_6H_{10}O_5]_n + nH_2O \longrightarrow C_6H_{12}O_6 \qquad (1)$$

Additional research has implemented the use of varying reactor types for improving glucose yields and the possibility of producing an up-scale model. Tjerneld et al. (1991) combined the individual pretreatment and reaction steps into one single process through employment of an attrition bioreactor (ABR)[37]. The ABR consisted of an agitator with a pitched-blade turbine impeller housed in a reactor vessel and milling media composed of 0.476 cm stainless steel balls. An aqueous two-phase system was also employed for enzyme recycling using water-soluble polymers for the bottom phase. The cellulase enzyme showed an obvious increase in activity when employed in the ABR with a two-phase system as opposed to using only a buffered solution. The ABR system also displayed a drastic increase in reducing sugar yields when compared to a conventional stirred-tank reactor[37]. Another method, performed by Karube et al. (1977), employed the use of immobilized cellulases suspended in packed-bed and fluidized bed reactors, with both reactor types displaying favorable results (in terms of sugar production) over native cellulase alone[38].

All research mentioned thus far has demonstrated various forms of the same basic principle for cellulose hydrolysis. This process has been perfected and is well-known throughout the

scientific community. Altercations arise in regards to the nature of the enzyme itself. The water solubility aspect of cellulase only permits it to be used once in a reaction and then discarded, which presents a major problem considering that the cost of the enzyme is approximately 70 cents per gallon of ethanol produced from lignocellulosic biomass, in capital costs[39]. In this regard, much research has been geared toward enzyme recovery methods which will allow for recycling. Various recovery methods include readsorption onto fresh substrate[14, 40], membrane ultra-filtration[16, 41-43], gel encapsulation[44], and immobilization onto various supports such as glass[45, 46], magnetic materials[4, 47-52], or polymeric materials[47, 53-60].

2.4 Enzyme Immobilization

Of the various techniques mentioned previously, immobilization of the cellulase enzyme appears to have the highest potential; this is due to several advantages which include enhanced stability, easy separation from reaction mixture, possible modulation of the catalytic properties, and easier prevention of microbial growth[61]. According to Garcia et al. (1989) the general attachment methods used in enzyme immobilization include physical adsorption to a solid phase, covalent bonding to a solid phase, covalent bonding to soluble polymers, cross-linking with bi-functional reagents, inclusion in a gel phase, and encapsulation[47]. One study by Johnson et al. (2007)bound a haloalkane dehalogenase (DhlA) enzyme to magnetic nano-particles by affinity-adsorption and found that the activity was significantly less when compared to the covalently linked DhlA particles[51]. Although physical adsorption is the simplest method, it is not recommended for cellulase enzyme immobilization as desorption is likely to occur during reactions followed by re-adsorption of the enzyme onto the substrate surface. Cellulase adsorption studies have indicated that EG's and CBH's readily adsorb to cellulosic materials and maintain a strong bond[62, 63].

One study by Takimoto et al. (2008) encapsulated cellulase enzyme within mesoporous silica (SBA-15) at varying pore sizes[64]. The highest activity retained was 65% of the free enzyme activity and was a result of encapsulation in a smaller pore size sample. It is believed that with the smaller pore size, the enzyme was immobilized closer to the silica surface, thus allowing better accessibility to substrate. Another study by Ge et al. (1997) immobilized cellulase and glucose isomerase within macroporous *p*-trimethylamine polystyrene beads using a molecular deposition technique[65]. The co-immobilized enzyme retained only 50% of its original activity after 4 recycles of 5 hours each; the immobilized enzyme activity was not compared to free enzyme activity. Encapsulation, either in a gel or some other porous material, would require that the substrate be completely solubilized in order to penetrate and reach the enzyme. When considering cellulose hydrolysis, however, the substrate is insoluble in water.

Much research has demonstrated that covalent bonding provides the most efficient and reliable method for enzyme reactivity with substrate and eventual recovery [47, 49, 50, 52]. Enzymes are typically bonded to support surface via surface functional groups; most notable are amine and carboxyl groups. This type of bond maintains a tight attachment with the enzyme and remains strongly attached after adsorption of substrate, which is in direct contrast to enzyme immobilization via physical adsorption techniques. Feng et al. (2006) immobilized a nonspecific chitosan hydrolytic enzyme (cellulase) onto magnetic chitosan microspheres for the purpose of preparing a water-soluble low-molecular-weight chitosan[66]. It was determined that the immobilized cellulase had retained 78% of its original activity after 10 hydrolytic recycles and remained more stable over time and over a broader range of temperature and pH than that of free cellulase. Chen and Liao (2002) also produced similar results due to immobilization of yeast alcohol dehydrogenase (YADH) on to magnetic nanoparticles[49]. Residual activity obtained was

62%, which was much higher than another method for alcohol dehydrogenase reported by Shinkai et al. (1991) (12%)[67], and also had excellent reusability in that it was recycled 13 times within 2 hours with no significant loss in activity. A separate study by Gao et al. (2003) immobilized B-lactamase I on colloidal stable silica encapsulated nano-magnetic composites and found that more than 95% of the original activity was retained after its first re-use[68].

Due to the high success rate consistently portrayed through covalent bonding, the study conducted for this research thesis has employed a covalent attachment approach to a solid support.

2.4.1 SPION

Superparamagnetic iron oxide nanoparticles (SPION) offer attractive possibilities over their larger micron-size counterparts. Over the past decade, nano-sized magnetic particles have received increasing attention with the rapid development of nanostructured materials and nanotechnology in the fields of biotechnology and medicine[69, 70]. One attractive aspect is that their size gives them dimensions comparable to those of a virus (20-500 nm), a protein (5-50 nm), or a gene (10-100 nm)[71]. Critical parameters are often required of these nanomagnets, which are most often noted in medical practice, and may include particle size, surface characteristics, and good magnetic response[71]. In recent years, they have been used in multiple biotechnological applications, including separation, detection, and magnetic resonance imaging.

2.4.2 Advantages of SPION's

The use of magnetic nano-particles as the support of immobilized enzymes has particular advantages which set them apart from other well-known support matrices. These include, but are not limited to, (1) higher specific surface area obtained for binding of a larger amount of enzyme, (2) lower mass transfer resistance and less fouling, and (3) immobilized enzymes can be

selectively separated from a reaction mixture by the application of a magnetic field[72]. Of particular interest is that once they are removed from an external magnetic field they are less likely to retain residual magnetism as compared to larger magnetic supports with similar properties[73, 74].

3 MATERIALS AND METHODOLOGY

3.1 Materials

A cellulase preparation was provided by Genencor (Rochester, NY). The enzyme solution was in crude form and used directly. Ammonium hydroxide, Rochelle salts (Na-K tartarate), Na-metabisulfite, citric acid monohydrate, and D-glucose were purchased from Fisher (Fair Lawn, NJ). Ferrous chloride tetrahydrate and ferric chloride were the products of Fluka (Buchs) and Sigma (St. Louis, MO), respectively. Polystyrene-coated amino superparamagnetic microparticles (1-2 μm) were purchased from Polysciences, Inc. (Warrington, PA). 3,5 Dinitorsalicylic acid, microcrystalline cellulose substrate, tetracycline, and cycloheximide (10 mg/ml) were the guaranteed reagents of Sigma. Sodium hydroxide and 1-(3-Dimethylaminopropyl)-3-ethylcarbodiimide hydrochloride (EDC) were supplied by E. M. Science (Cherry Hill, NJ) and Merck (Germany), respectively. Bio-Rad reagent for protein assay was obtained from Bio-Rad Laboratories (Hercules, CA). The water used throughout this study was de-ionized and filtered using a U.S. Filter purification system.

3.2 Methods for Immbolization and Recycling of Magnetic Particles

3.2.1 Preparation of Magnetite Nanoparticles

Magnetite nanoparticles (Fe_3O_4) were prepared by co-precipitating Fe^{2+} and Fe^{3+} ions by ammonia solution and treating under hydrothermal conditions[75, 76]. A 2:1 molar ratio of ferric and ferrous chlorides was dissolved in nanopure water under anoxic conditions. Chemical precipitation was achieved at 25°C under vigorous stirring by adding 28% NH_4OH solution. The precipitates were heated to 80°C for 30 minutes, and then washed three times with water and one time with anhydrous ethanol. The particles were then dried by purging with nitrogen for 24 hours and recovered.

3.2.2 Cellulase Immobilization

For binding of the cellulase enzyme complex, 120 mg of magnetite nanoparticles were added to a solution containing 8 mg/ml carbodiimide (EDC). The mixture was then sonicated for 3 minutes and refrigerated for 30 minutes until the temperature reached 4°C. 1 ml of crude enzyme solution (8 mg/ml protein in de-ionized water) was then added and followed with sonication for 3 minutes. The reaction mixture was stored at 4°C and sonicated for an additional 3 minutes at regular time intervals to ensure uniform dispersion. After 24 hours, the mixture was sonicated a final time (for the same duration as previously listed) and then heated to 25°C. The cellulase-bound nanoparticles were recovered by placing the container on a strong permanent magnet. They were washed two times in de-ionized water and the resultant supernatants were used for protein analysis. The nanoparticles would then proceed to be measured for activity, recyclability, and stability. For immobilization of the polystyrene-coated magnetic particles, 4 ml of solution containing 2.5% solids in water were added to a solution containing 8 mg/ml carbodiimide (EDC). The binding procedure was then carried out under the same conditions as the magnetite nanoparticles.

3.2.3 Analysis of Reducing Sugars

3,5 Dinitrosalicylic acid (DNS) is an aromatic compound which reacts with reducing sugars and other reducing compounds to form 3-amino-5-nitorsalicylic acid, which absorbs light strongly at 540 nm[77]. The DNS method was used in this study to determine the amount of glucose formed as reducing sugars resulting from a reaction with dinitrosalicylic acid reagent. D-glucose was used as the standard. High-Performance Liquid Chromatography (HPLC) is a well-known separations technique for identifying key compounds in aqueous solution. Selected samples from this study were also analyzed using HPLC in order to confirm glucose production

and identify additional compounds present (i.e. cellobiose, xylose, etc.). Analysis was conducted using an Agilent 1200 isocratic HPLC system equipped with a differential refractive index detector (RID) and using a Bio-Rad Aminex HPX-87P column (300 X 7.8 mm, 9 µm particles, 1.0 ml/min, 80˚C).

3.2.4 Activity and Stability Measurements

The enzymatic activity was determined by measuring glucose production after a reaction of cellulase-bound magnetic particles with microcrystalline cellulosic substrate. Following 96 hours of hydrolysis, a 0.5 ml aliquot of the reaction supernatant was removed and added to 3 ml of DNS reagent to stop the reaction. The samples were heated in a boiling water bath for 5 minutes to allow color formation. They were then cooled and centrifuged. The reducing sugar concentration in the resulting supernatant was then measured at 540 nm on a Genesys 20 single beam spectrophotometer. Unless otherwise stated, the activity of free enzyme was measured following similar procedures and conditions as stated for the bound cellulase complex.

The thermal stability of the immobilized cellulase complex was determined by measuring the activity as a function of time at an optimum temperature of 50°C. The samples contained 120 mg of immobilized enzyme and 0.2 g of microcrystalline cellulose in 20 ml of 0.05M citrate buffer (pH 5.0) and de-ionized water. Reducing sugar concentrations were measured as reducing sugars at specified time intervals throughout the reaction using the DNS assay.

3.2.5 Recyclability of Enzyme-bound Nanoparticles

The reusability of cellulase-bound magnetic particles was demonstrated by measuring the reducing sugars produced from a reaction of the particles with substrate over a time period of 96 hours. Enzyme-bound nanoparticles (120 mg) were added to a solution containing 0.2 g of microcrystalline cellulose, 80 µl of tetracycline, 60 µl of cycloheximide, 10 ml of citrate buffer

(0.05 M, pH 5.0) and enough de-ionized water to bring the total volume to 20 ml. Following the specified reaction time, the particles were magnetically separated and introduced on to fresh cellulosic substrate. After each 24 hour time period, 0.5 ml of the supernatant was removed to determine reducing sugar production over time and demonstrate its stability. The enzymatic activity was measured and recorded after 96 hours of hydrolysis.

A series of blanks were coincidentally measured in order to compensate for any interference, one containing enzyme alone and another containing substrate alone. Any response measured by the spectrophotometer from these blanks was subtracted from the primary hydrolysis reaction to obtain an accurate measurement. All samples were measured in triplicate to increase accuracy.

3.3 Methods for Characterization of Magnetite NanoparticlesCharacterization

The size and morphology of iron oxide nanoparticles were determined by Transmission Electron Microscopy (TEM) using a JEOL 100-CX electron microscope. The binding of the cellulase complex to the nanoparticle surface was determined using a Bradford protein assay. The bound enzyme (measured as protein) was calculated by the difference between the original protein solution added and the protein found in the removed supernatant. It was measured by a colorimetric method involving the binding of Coomassie Brilliant Blue G-250 to the protein and then measuring the concentration across a wavelength of 595 nm[78]. Bio-Rad dye reagent was used for the protein assay and bovine serum albumin as the standard. Although the cellulase enzyme complex used for this research may contain proteins that are not enzymes, it was assumed for this research, that the enzyme-to-protein mass ratio remains fairly constant. This assumption was critical for assuming that Bradford assay results were representative of enzyme quantity. As this particular cellulase preparation is a crude enzyme complex, the specific ratio was not available. The binding of the enzyme was confirmed by Fourier Transform Infrared

(FTIR) Spectroscopy using a Thermo Nicloet Nexus 670 FTIR model and by X-ray Photoelectron Spectroscopy (XPS) using a Kratos Axis 165 XPS/Auger.

3.3.2 Optimization

The binding efficiency of enzyme to magnetic nanoparticles was determined by first evaluating the saturation of the cellulase enzyme complex on the surface of the precipitates. Subsequently, the ideal weight ratio (weight of enzyme : weight of nanoparticles) was then determined in order to find the optimum condition allowing for maximum activity.

The effect of pH on activity was evaluated using buffers of various pH values. For pH 3, 0.1 M potassium phthalate buffer was used. For pH 4, 0.1 M sodium acetate buffer was used. For pH 5, 0.05 M citrate buffer was used. For pH 6, potassium phosphate buffer was used; and sodium phosphate buffers were used for pH 7 and 8. Hydrolysis reactions were performed using 8.57 mg of enzyme-bound nanoparticles, 50 mg of microcrystalline cellulose, and 1 ml buffer.

For the optimum temperature study, various temperatures were examined spanning a range from 25°C – 80°C and the corresponding activity was measured for each. Similar reactor conditions were implemented for this study as were demonstrated with the pH optimization, except that 1 ml of 0.05 M citrate buffer (pH 5.0) was used for all hydrolysis reactions.

3.3.3 Activity Measurements

The enzymatic activity was determined by measuring reducing sugar production after a reaction of enzyme-bound nanoparticles with microcrystalline cellulose. After initial binding, 0.5 ml of the well-mixed solution containing 8.33 mg of enzyme-bound particles was added to 50 mg of cellulosic substrate and 1 ml of buffer (0.05 M citrate buffer, pH 5.0). The resulting mixture was allowed to incubate at 50°C for 1 hour, after which 3 ml of DNS reagent was added immediately to stop the reaction. The samples were heated in a boiling water bath for 5 minutes

to allow color formation. They were then cooled and centrifuged for an additional 5 minutes. The reducing sugar concentration in the resulting supernatant was then measured over a wavelength of 540 nm on a Genesys 20 single beam spectrophotometer. In order to compensate for any interference, a series of blanks were measured in the same manner, one containing enzyme alone and another containing substrate alone. Any response measured by the spectrophotometer from these blanks was subtracted from the primary hydrolysis reaction to obtain an accurate measurement. Unless otherwise stated, the activity of free enzyme was measured following similar procedures and conditions as stated for the bound cellulase complex.

4 PREPARATION AND CHARACTERIZATION OF CELLULASE-BOUND MAGNETITE NANOPARTICLES (SPION)

4.1 Results and Discussion

4.1.1 Nanoparticle Size and Morphology

The TEM images of magnetic nanoparticles without (a) and with (b) immobilized cellulase enzymes are shown in Figure 4.1 along with their corresponding size distributions. The pure Fe_3O_4 particles appear to be fairly monodisperse with a mean diameter of 13.28 $\pm$ 3.9 nm.

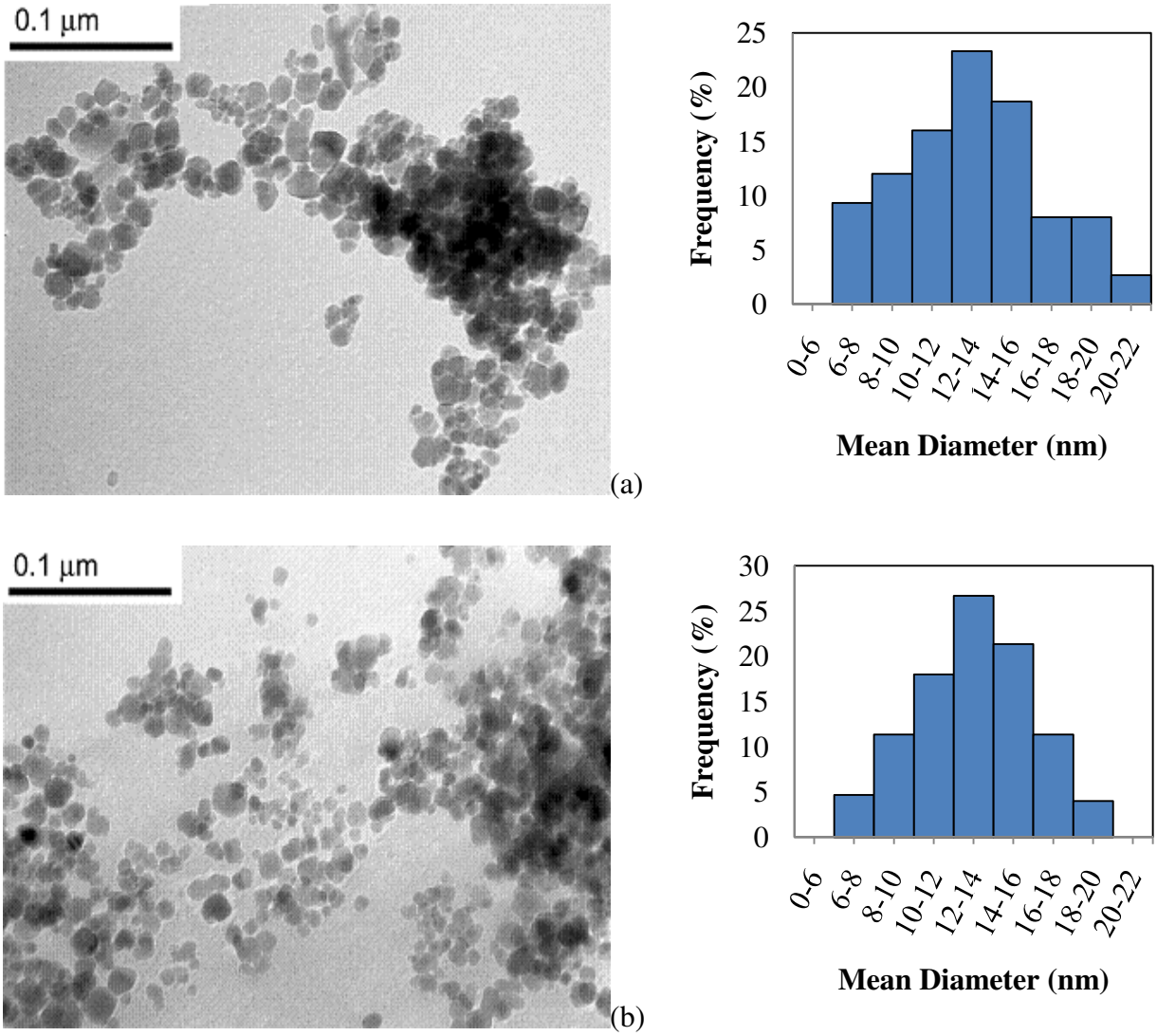

Figure 4.1: Transmission electron microscopy (TEM) images of magnetic nanoparticles (a) before and (b) after cellulase immobilization. Weight Ratio (Enzyme solution/Fe_3O_4) = 0.028 (w/w).

After binding of the cellulase enzyme, the nanoparticles remained discrete and had a mean diameter of 13.31 $\pm$ 3.2 nm. Upon inspection of the micrographs, 150 particles were randomly chosen for statistical analysis to determine if there was any significant difference in size between the bare iron oxide nanoparticles and the nanoparticles containing the bound cellulase enzyme complex. A 95% confidence interval was constructed indicating that the difference between the two population means was most likely in the range (-0.402, 0.432). This analysis suggests that the binding process did not cause any significant change in size ($\alpha = 0.05$, p-value = 0.976); and, from physical inspection of the images, it is noticeable that no additional aggregation occurred as a result. The minimal change in size is indicative of a very low enzyme loading.

4.1.2 Mechanism for Enzyme Immobilization

The binding of the cellulase enzyme complex to magnetite nanoparticles was confirmed by FTIR and XPS. Figure 4.2 shows the FTIR spectra for the solid state crude enzyme preparation, naked Fe_3O_4 nanoparticles, and enzyme-bound Fe_3O_4. The characteristic bands at 1653 and 1542 cm^{-1} on the cellulase enzyme complex are also present on the nanoparticles containing immobilized cellulase, therefore confirming attachment of the enzyme to Fe_3O_4 nanoparticles. A shift in frequency from 1542 cm^{-1} to 1522 cm^{-1} on the immobilized enzyme is likely due to the formation of an amide bond (Figure 4.3) resulting from the reaction between a carboxyl group on the enzyme and an amine group on the nanoparticle surface. The frequency shift is caused by stretching of the C=O bond and additional –NH bending vibration. The naked Fe_3O_4 nanoparticles also show a characteristic band at 1618 cm^{-1} which may be due to bending of the amine functional group. This peak is no longer present with the immobilized cellulase enzyme, further indicating an amide bond formation. The weaker bands for the immobilized cellulase are essentially a result of low enzyme loading on the nanoparticle surface.

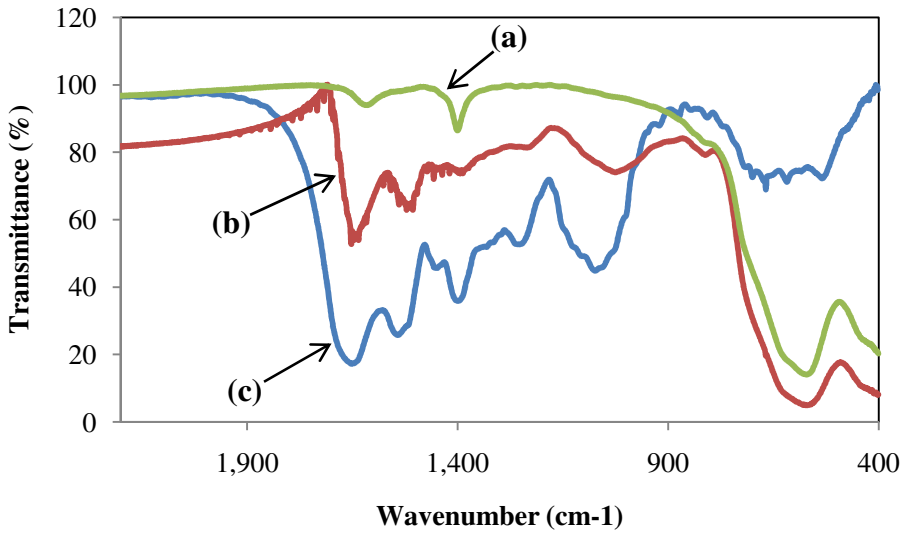

Figure 4.2: FTIR spectra of magnetite nanoparticles without (a) and with (b) bound cellulase, and free cellulase enzyme complex (c).

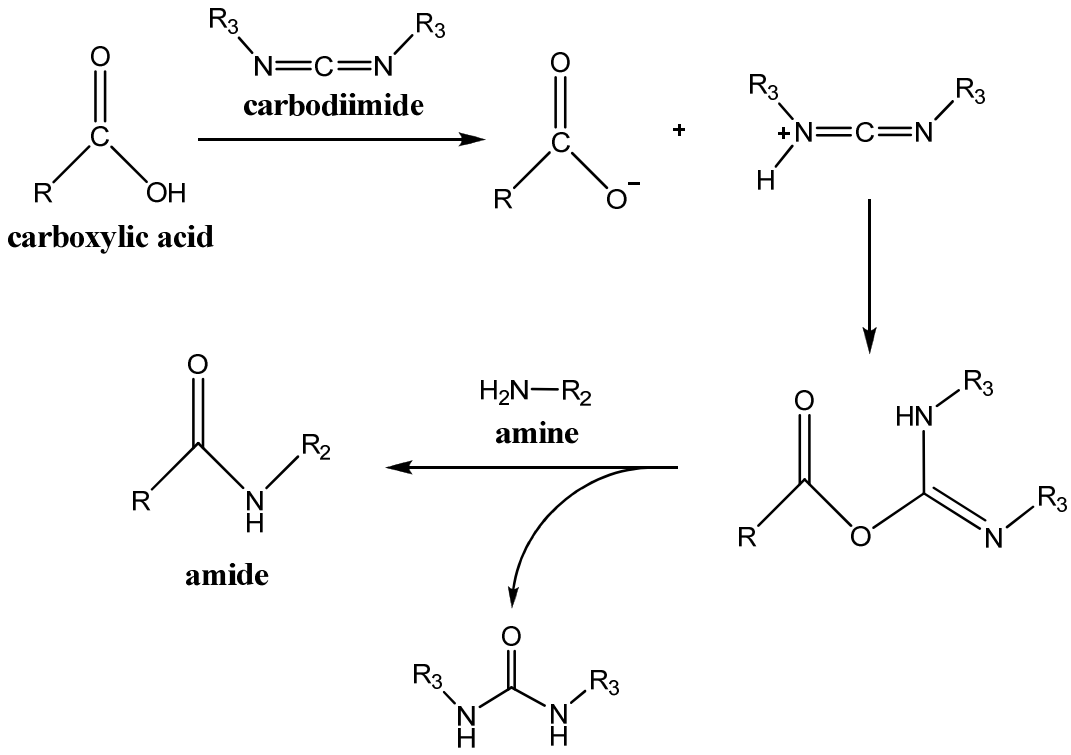

Figure 4.3: Synthesis involving amide bond formation via carbodiimide activation.

Figure 4.4 displays an XPS spectrum for samples containing pure Fe_3O_4 nanoparticles and Fe_3O_4 nanoparticles with the cellulase complex attached. Characteristic peaks at 398.6 and 284.6 eV on the enzyme-bound nanoparticles indicate a heavy loading of nitrogen and carbon which are not present on the unbound nanoparticles. This confirms attachment of the enzyme complex as this increase in nitrogen and carbon can be attributed to the amine and carboxyl groups found on the cellulase enzyme.

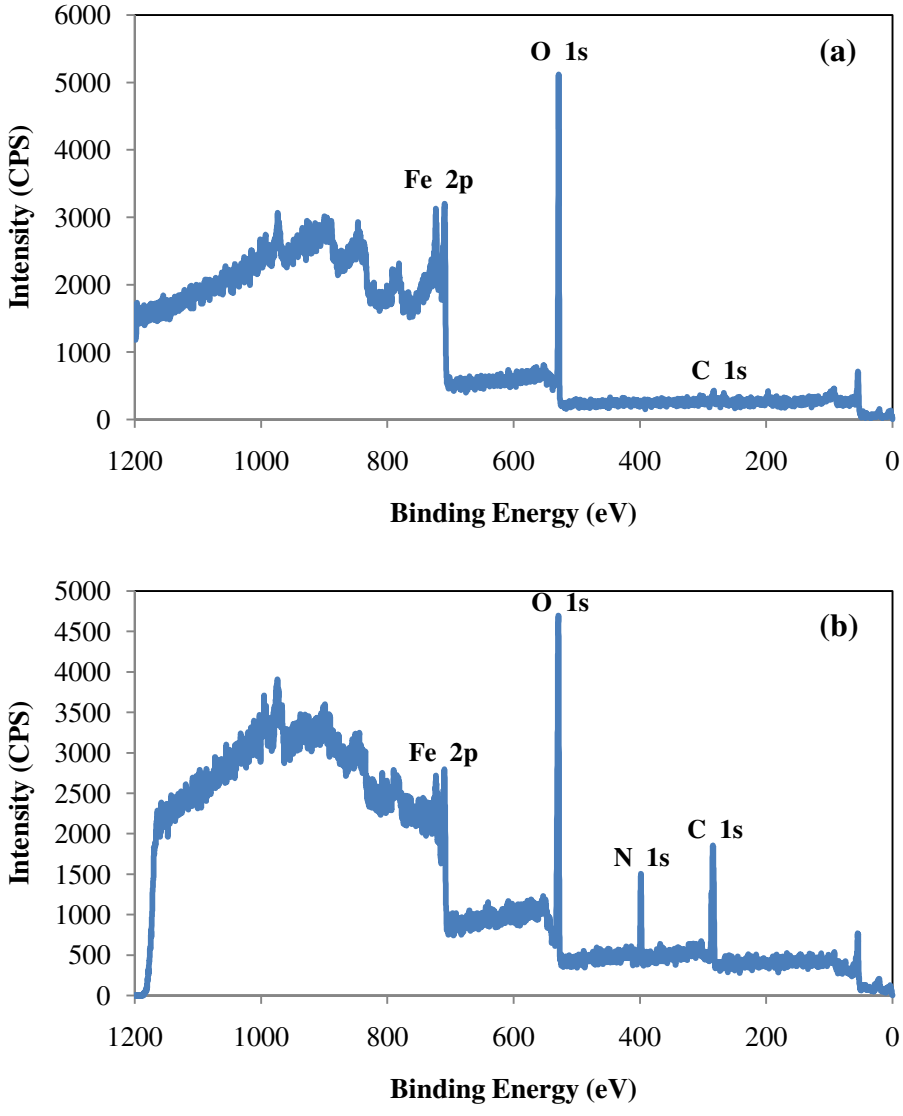

Figure 4.4: (a) XPS analysis of pure Fe_3O_4 nanoparticles and (b) cellulase-bound Fe_3O_4 nanoparticles.

Of particular interest are the concentrations of the individual elements which are shown in Table 4.1. An atomic concentration of 39.51% for carbon on the enzyme-bound nanoparticles results in a 15.8% increase from the unbound nanoparticles. The atomic concentration of nitrogen increased to 8.13% on the enzyme-bound nanoparticles, whereas there were none detected on the unbound nanoparticles. Also shown are the characteristic proportions of iron and oxygen which are of similar proportions for both samples.

Table 4.1: Elemental analysis of pure and enzyme-bound Fe_3O_4 from evaluation by XPS.

	Peak	Position BE (eV)	FWHM (eV)	Raw Area (CPS)	RSF	Atomic Mass	Atomic Concentration (%)	Mass Concentration (%)
Pure Fe_3O_4	Fe 2p	709.1	4.570	36688	2.957	55.85	54.74	81.38
	C 1s	283.6	1.638	466.5	0.278	12.01	6.240	2.000
	O 1s	528.7	1.376	7554	0.780	16.00	39.02	16.62
Enzyme-Bound Fe_3O_4	Fe 2p	709.8	4.607	29652	2.957	55.85	22.74	54.46
	C 1s	284.6	3.259	5742	0.278	12.01	39.51	20.34
	N 1s	398.6	1.815	1962	0.477	14.01	8.130	4.880
	O 1s	529.1	2.711	11156	0.780	16.00	29.61	20.31

4.1.3 Binding Efficiency

By assaying the amount of protein found in the supernatant after the enzyme binding process, it was determined that when the amount of Fe_3O_4 nanoparticles was kept constant at 50 mg, the results displayed a higher level of bound enzyme (measured as protein) when low enzyme loadings were administered. The maximum amount of bound enzyme was more than 90% when 1 mg of enzyme complex was added at the initiation of the reaction. The percentage of bound enzyme decreased exponentially as the amount of enzyme added was increased from 1 mg to 18 mg. This is depicted in Figure 4.5.

4.1.4 Enzyme Optimization

By assaying the amount of unbound enzymes (measured as protein) in the supernatant after immobilization and measuring their corresponding activity, the optimum weight ratio of

bound enzyme to nanoparticles was determined. An initial loading of 50 mg of magnetic Fe_3O_4 was kept constant for this process and enzyme loading was increased, as was carried out with the determination of binding efficiency. The maximum weight ratio achieved was determined to be 0.16.

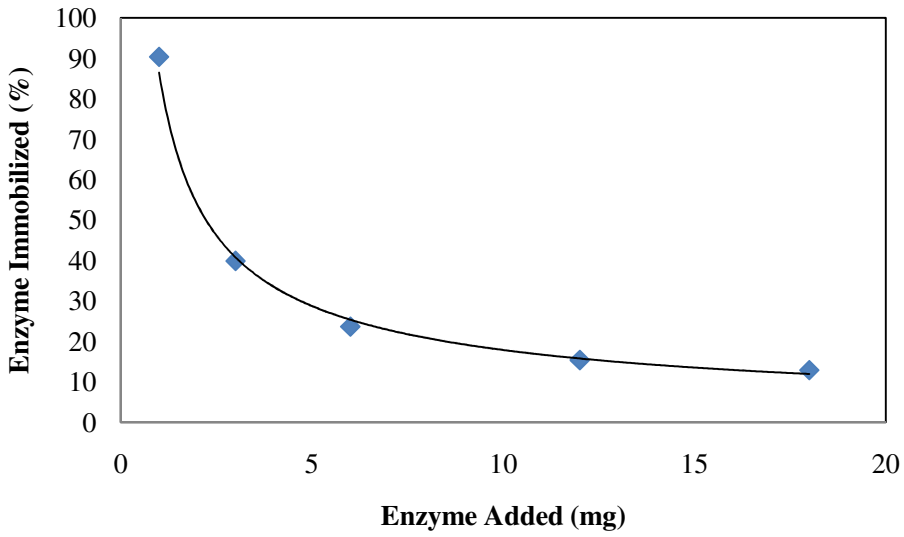

Figure 4.5: Binding Efficiency for varying amounts of protein added to 50 mg of Fe_3O_4 nanoparticles

It has been proposed that enzyme which is too heavily saturated upon the surface of the nanoparticles will, in effect, hinder itself by blocking active binding sites from reaching the substrate and, therefore, causing an overall reduction in activity. As shown in Table 4.2, the point of saturation for the enzyme complex on the nanoparticle surface appears to be 0.02 as it attained a maximum activity value of 62.7 µmol glucose/mg-hr. The relative activity curve for the varying weight ratios is shown in Figure 4.6.

The pH dependency of an enzyme is dependent on the nature of its functional groups. The total charge on an enzyme's active sites determines if the enzymes optimum operability will result from an acidic or basic microenvironment. However, coupling of an enzyme to a support, whether charged or uncharged, will typically cause a shift in the ideal pH. Generally, the greater

Table 4.2: Activity values for varying ratios of bound cellulase enzyme to Fe_3O_4 nanoparticles.

Cellulase Added (mg)	Cellulase Bound (mg)	Weight Ratio (mg bound enzyme / mg nanoparticles)	Activity (µmol glucose / mg enzyme-hr)	Relative Activity (%)
0	0	0	0	0
1	0.782	0.016	40.14	63.97
3	1.042	0.021	62.75	100
6	1.409	0.028	33.07	52.70
18	2.722	0.054	25.42	40.51
21	4.181	0.084	22.96	36.59
25	7.973	0.159	12.16	19.37

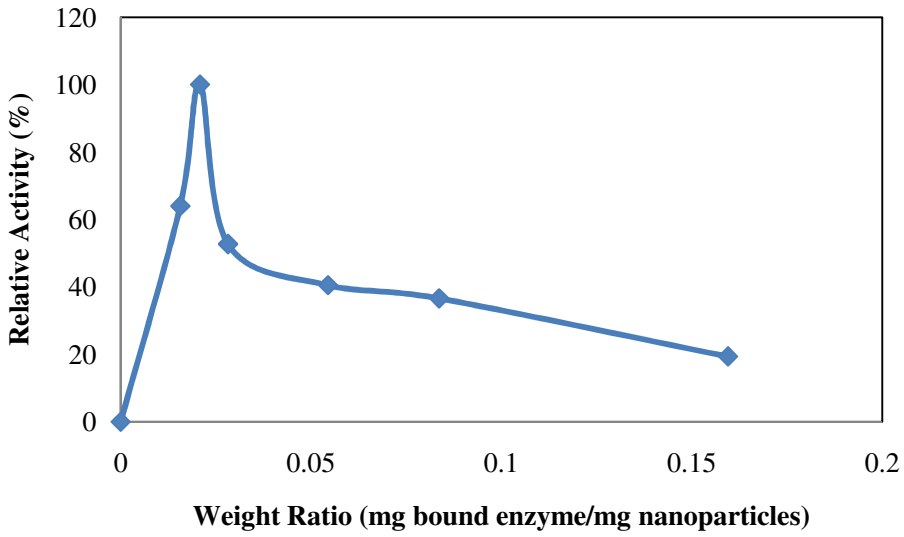

Figure 4.6: Relative Activity values corresponding to immobilized enzyme weight ratios.

the charge on the support, the greater the effect, particularly if the substrate is charged as well[79, 80]. The binding protocol for this experiment used positively charged amino groups for immobilization, therefore an alteration in the ionic atmosphere and total shift in the optimum pH was expected. As shown in Figure 4.7, the maximum activity for immobilized cellulase complex occurred under a pH of 5.0, which indicates an increase in net negative charge of the immobilized enzyme as compared to an optimum pH of 4.0 for the free enzyme. The pH of the microenvironment becomes lower than that of the bulk solution as a result.

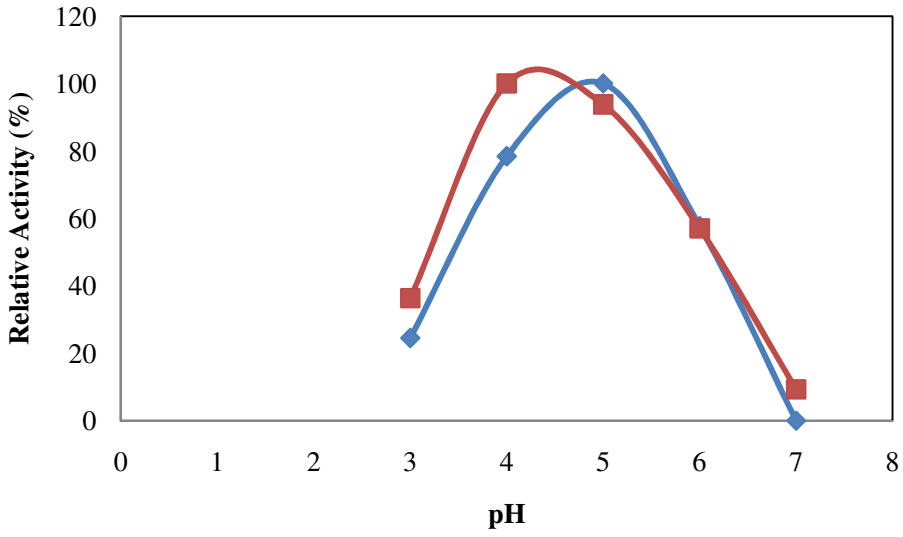

Figure 4.7: Effect of pH on activity of free and immobilized cellulase at 50˚C.

Immobilization of an enzyme can cause changes in its thermal characteristics which will generally incite an apparent improvement in stability. However, an increase in temperature can also increase protein denaturation, which can occur as a result of changes in tertiary structure, oxidation of some labile groups, or some other physical modification of the protein[81]. In effect, activity is reduced along an exponential decay. The immobilized cellulase complex demonstrated an optimum activity at a temperature of 50°C.

As shown in Figure 4.8, the immobilized cellulase displayed a high activity over a broader range of temperatures compared to the free enzyme. Disruption of weak intramolecular forces and subsequent unfolding of the protein chain in free enzymes can be caused by thermal deactivation[47]. Immobilization of the cellulase complex increased the thermal stability by stabilizing the weak ionic forces and hydrogen bonds thus increasing the range of operating temperatures.

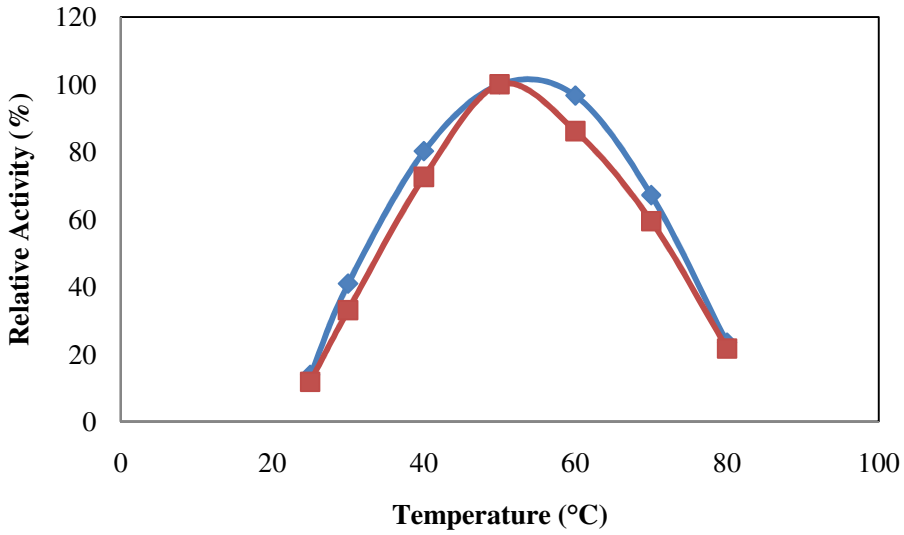

Figure 4.8: Effect of temperature on activity of free and immobilized cellulase at pH 5.0.

4.2 Conclusions

A crude cellulase enzyme complex was successfully immobilized on magnetic Fe_3O_4 nanoparticles via carbodiimide activation and characterized. The pure Fe_3O_4 particles were analyzed using TEM and were determined to have an average diameter of 13.28 nm $\pm$ 3.9 nm. Enzyme-bound particles showed no significant change in size and it was determined that no additional agglomeration occurred due to the binding process. Enzyme attachment was confirmed using FTIR and XPS. Enzymatic activity was determined by measuring glucose as reducing sugars using the DNS method. Saturation of the cellulase enzymes on a magnetic support is useful for determining maximum binding ability without further hindering enzymatic

activity. Maximum efficiency for enzyme-to-support binding was verified at low enzyme loadings and the saturation point was confirmed at a weight ratio of 0.02. Ideal operating conditions were evaluated for pH and thermal stabilities. The optimum pH shifted from 4.0 to 5.0 after immobilization and the optimum temperature was 50°C. Immobilized cellulase was demonstrated to have greater stability over a wider range of temperatures as compared to free enzyme.

5 RECYCLABILITY OF CELLULASE ENZYME IMMOBILIZED ON MAGNETITE NANOPARTICLES DURING CELLULOSE HYDROLYSIS

5.1 Results and Discussion

5.1.1 Recyclability

The recyclability of immobilized cellulase enzymes were determined by measurement of the total reducing sugars produced over time and following with magnetic separation, after which new substrate would be introduced. This is demonstrated in Figure 5.1, which displays the reduction in reducing sugars after each recycle as a result of a loss in enzymatic activity. The activity of immobilized enzyme was determined to be 30.2% of the free enzyme activity following the initial hydrolysis reaction.

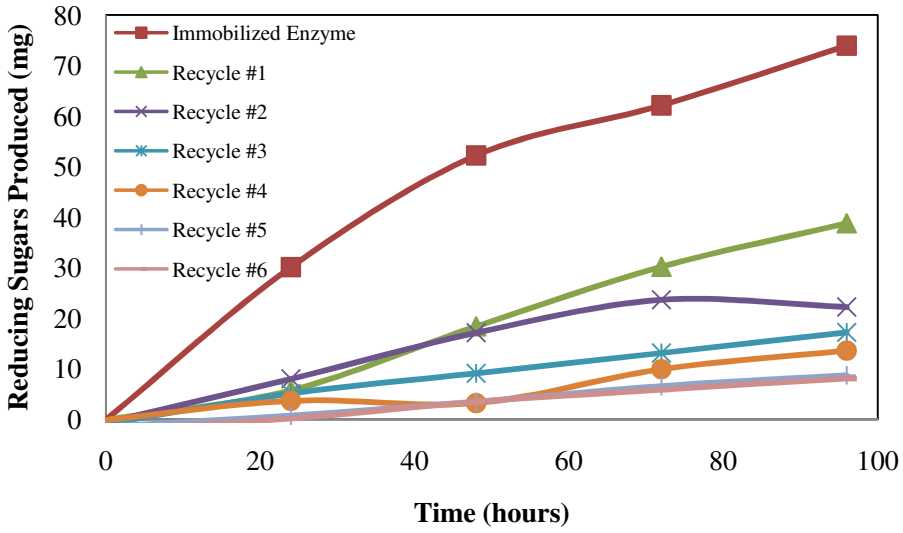

Figure 5.1: Reducing sugar production over time for immobilized enzyme through 6 recycles.

The enzyme complex was recycled a total of six times before the residual activity had fallen to approximately 10% of the initial. Table 5.1 gives the data values for the reducing sugars produced and there corresponding activity values following each immobilized enzyme recycle. Figure 5.2 shows the retention of activity for the immobilized cellulase complex. An apparent loss in activity was observed following each recycle with the majority (47.5%) being

lost following the initial reaction. This resultant loss in activity could be attributed to several factors, which may include protein denaturation, end-product inhibition, and/or loss of one or more individual components of the cellulase complex. Another possible reason could be modification of the enzymes structure due to carbodiimide activation. The individual enzymes composing the cellulase complex each contain a large number of functional groups available for immobilization, many of which are located on the active site of the enzyme and are specific to cleaving the individual linkages between glucose monomers of the cellulosic substrate. Should one of the functional groups located on the active site of the enzyme be used for immobilization, a large decrease in stability could result and it's possible the enzyme could be destroyed in the harsh environment of the hydrolysis reaction[4].

Table 5.1: Hydrolysis of recycled immobilized enzyme and resulting activity values.

Recycle #	Hydrolysis Time (days)	Reducing Sugars Produced (mg)	Enzymatic Activity (μmol/mg-hr)	Relative Activity (%)
0	4	73.89	1.010	100.0
1	8	38.77	0.530	52.47
2	12	22.23	0.304	30.09
3	16	17.22	0.235	23.30
4	20	13.61	0.186	18.42
5	24	8.760	0.120	11.86
6	28	8.110	0.111	10.98

When comparing the performance of the enzyme-bound nanoparticles over all 6 recycles to that of the free enzyme it was determined that, after 24 hours of hydrolysis, the nanoparticles produced 94.5% of the sugars produced by free enzyme. The total sugars produced by the enzyme-bound nanoparticles, as compared to free enzyme, are demonstrated in Figure 5.3. It should be noted that the 24 hour point covers the total reducing sugars produced for all recycles at each 24 hour mark of each recycle; meaning that the immobilized enzyme complex has already completed a complete 96 hour recycle before reaching the 24 hour point of the next and

subsequent recycles. Following all recycles, the efficiency of the immobilized enzyme complex dropped, producing 76.8% of the sugars produced by free enzyme following 96 hours of hydrolysis. Based on results from this research it appears that immobilization of the enzyme complex would not prove to be a cost-effective approach for hydrolyzing cellulose over long periods of time. However, future optimization experiments and/or modifications to methodology may significantly alter the outcome. The build-up of glucose and cellobiose is known to inhibit the performance of endoglucanases in the enzyme complex, and therefore, a better approach might be to stop the reaction after 24 hours and then recycle the enzyme-bound nanoparticles due to the high efficiency displayed early on in the reaction. This shorter interval would remove the enzymes from solution before high levels of end-products are formed.

Reducing sugars produced during hydrolysis were also evaluated by HPLC to determine glucose concentrations and measure accuracy of the DNS method. Selected samples were chosen for this analysis and their results are displayed in Table 5.2. Evaluation of these results reveals that the majority of the samples are glucose with minimal concentrations of xylose. Cellobiose was also detected in few samples at very low concentrations.

The data also reveals that the DNS analysis detects relatively fewer reducing sugars compared to the HPLC analysis. This could, in part, be attributed to discrepancies in sample preparation when the color formed DNS solutions were diluted to achieve more accurate readings by the spectrophotometer. In lieu of these variations, the majority of the samples from the two analytical methods displayed a difference less than 25%. Therefore, the method of using DNS for detection of reducing sugars was considered to be acceptable. When choosing a method for sugar analysis, HPLC would be considered as favorable over the DNS method. Although dilution of samples following color formation during DNS analysis is considered acceptable practice, there still remains a higher affinity for human error.

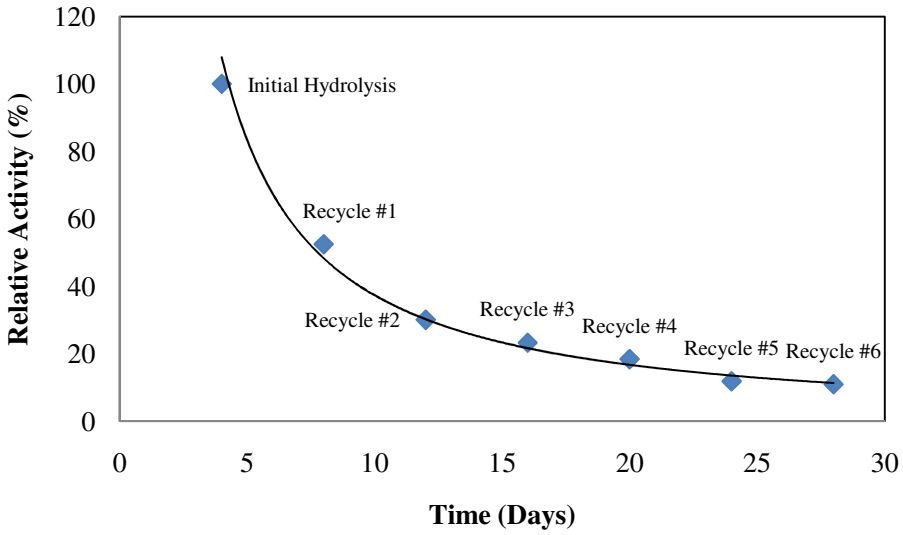

Figure 5.2: Retention of activity of immobilized cellulase enzyme following 6 recycles.

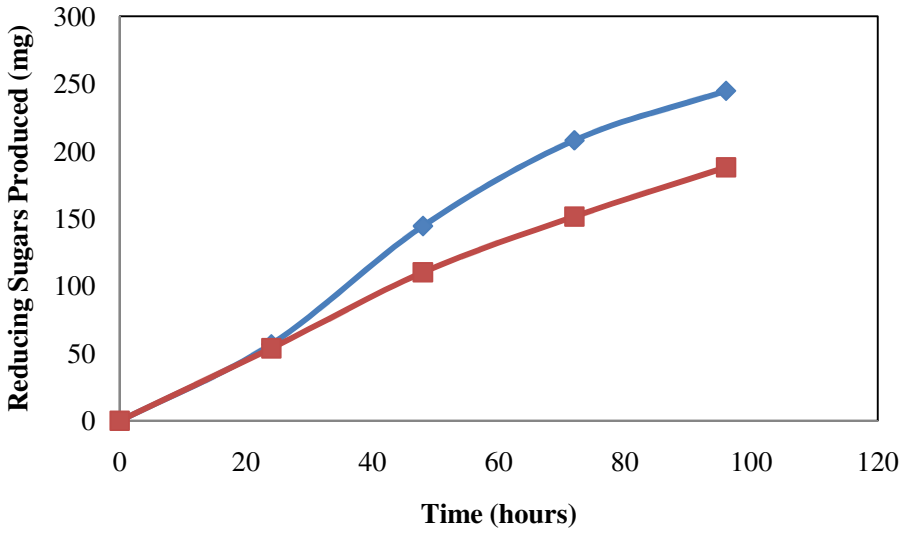

Figure 5.3: Total sugars produced by immobilized enzyme complex over 6 recycles with comparison to free enzyme.

HPLC also has the advantage of detecting individual sugar concentrations as opposed to total reducing sugars. The buildup of individual sugar molecules during hydrolysis would allow a better understanding of which enzymes in the complex remain active throughout the reaction.

Table 5.2: Compounds detected by HPLC analysis for selected sugar samples with comparison to reducing sugars detected by DNS.

Sample:	Glucose µg/g:	Xylose µg/g:	Total µg/g:	RS (DNS) µg/g:
1	1465	47	1512	1501.3
2	532	29	561	498.7
3	263	22	285	227.8
4	170	17	186	98.3
5	103	11	113	59.1
6	205	9	214	278.9
7	107	6	113	127.5
8	37	2	39	22.6
9	14	n/d	14	1.3

* RS = reducing sugars

A measurement of enzyme concentration (measured as protein), for the reaction following each recycle, suggested that the total loss in activity could also be attributed to detachment of enzymes from the support surface. The resulting loss is displayed in Table 5.3. The remaining enzymes (also shown in Table 5.3) give a more accurate indication of the true activity. Approximately 26% of the initially attached enzymes were physically lost before the first recycle, which may have resulted from a portion of weakly bound enzyme becoming detached once contact was made with substrate. A slower decay process followed. Figure 5.4 shows the corrected relative activity curve which only takes into account the remaining enzymes following each recycle. The original activity curve is also displayed for comparison. It is suggested that the weakly bound en zymes were not covalently bound as was expected from carbodiimide activation of the enzymes functional groups, but merely adsorbed on the support surface allowing them to become easily detached during the initial hydrolysis reaction.

5.1.2 Stability

Enzymatic activity was measured as function of time to determine the stability of the immobilized enzyme complex at 50°C. Figure 5.5 shows the thermal stabilities of immobilized and free cellulase enzymes. The enzyme bound nanoparticles showed a linear decrease in activity falling to 57.9% following 72 hours of hydrolysis. The free enzyme displayed a similar decay pattern, showing an activity of 51.2% after 72 hours. The immobilized enzymes decay rate remained relatively constant for 96 hours, at which point the activity had fallen to 43.4%.

Table 5.3: Enzyme (determined via protein assay) released from Fe_3O_4 nanoparticles and corrected reducing sugars produced as a result.

Recycle #	Enzyme Released (%)	Remaining Enzyme Attached (%)	Total Reducing Sugars Produced (mg)	Reducing Sugars per Remaining Enzyme (mg/mg)
0	25.979	74.021	73.895	23.769
1	35.389	64.611	38.772	14.288
2	45.820	54.180	27.684	12.166
3	53.166	46.834	17.216	8.752
4	58.977	41.023	13.609	7.899
5	63.384	36.616	8.763	5.698
6	64.509	35.491	8.115	5.444

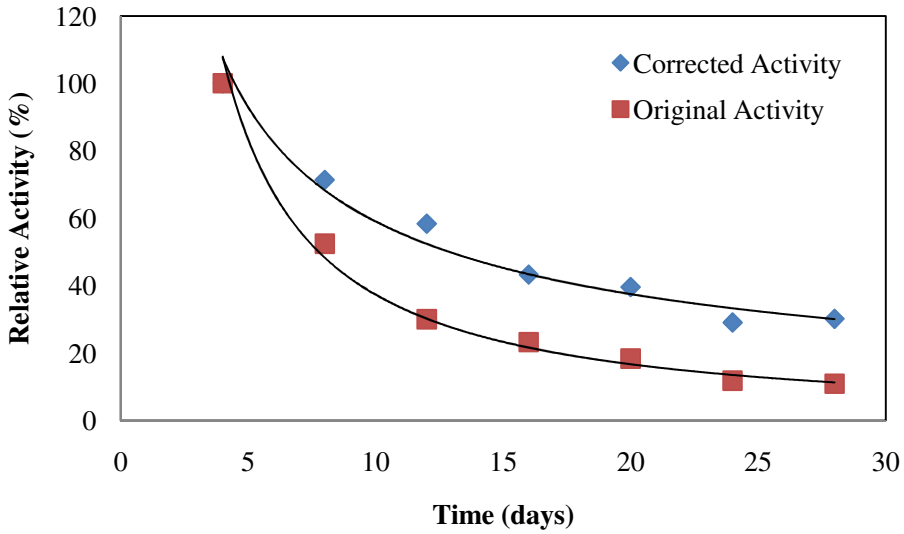

Figure 5.4: Relative activity of recycled immobilized enzyme corrected for enzyme detachment from Fe_3O_4 nanoparticles.

This was to be expected as the celluase complex was maintained in the original solution throughout the reaction, and the formation of glucose and cellobiose end-products would largely inhibit the enzymatic activity. The overall activity of the enzyme complex, therefore, was not hindered by immobilization and was shown to have a similar decay rate as compared to that of the free enzymes.

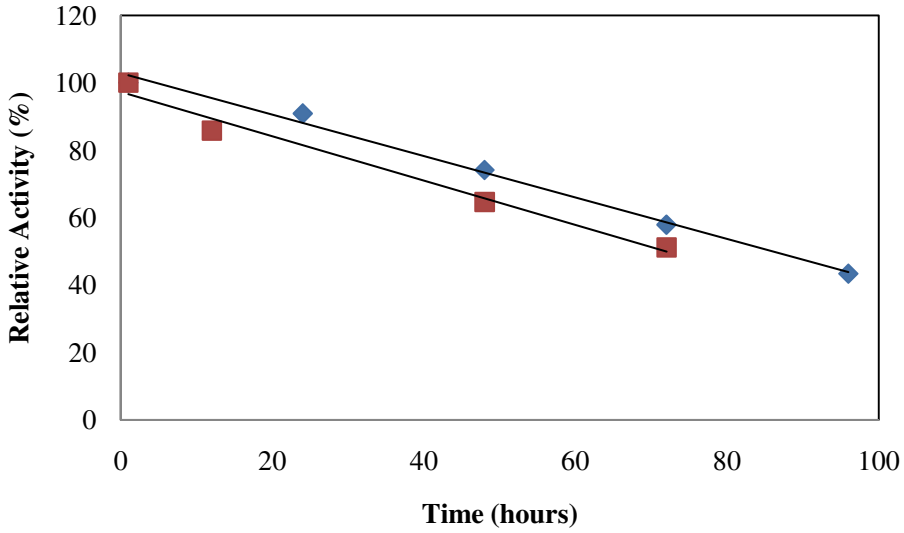

Figure 5.5: Thermal stability of immobilized and free cellulase at 50°C and pH 5.0.

5.2 Conclusions

A cellulase enzyme complex was covalently bound to the surface of magnetic Fe_3O_4 nanoparticles via carbodiimide activation and analyzed for stability and recyclability. Enzymatic activity was measured using the DNS method to determine glucose formation as reducing sugars and was confirmed with HPLC. The enzyme complex was recycled six times after which the resulting activity had fallen to 10% of its original value. Total sugars produced over 6 recycles by the enzyme-bound nanoparticles were only 76.8% of the free enzyme production, suggesting that immobilization by this procedure would not represent a cost-effective approach.

A protein assay demonstrated that the total loss in activity following each recycle could be partly attributed to enzyme detachment from the solid support, suggesting that not all enzyme

attachment resulted from covalent bonding but also from physical adsorption. The majority of activity loss, however, could be attributed to several factors, including protein denaturation, end-product inhibition, a loss in stability of one or more components of the cellulase complex, and/or modification of the enzyme structure due to carbodiimide activation of the enzymes carboxyl groups, to name a few. The immobilized enzyme complex was also demonstrated to have a slight advantage in stability when compared to free enzyme over the first 72 hours of hydrolysis with both enzyme complexes displaying similar decay rates.

6 CELLULASE IMMOBILIZATION ON POLYSTYRENE-COATED Fe_3O_4 PARTICLES AND EFFECTS ON RECYCLING DURING CELLULOSE HYDROLYSIS

6.1 Results and Discussion

6.1.1 Reusability

The reusability of a cellulase enzyme complex immobilized on polystyrene-coated microparticles was determined by measurement of reducing sugars produced from hydrolysis of cellulosic substrate after 96 hours, after which the particles were magnetically separated and introduced to fresh substrate. The particles reusability lasted over 4 recycles before the resulting enzymatic activity had fallen to 3.9%. The progress of each reaction was determined by measuring sugars produced at 24 hour time intervals during each recycle and is depicted in Figure 6.1.

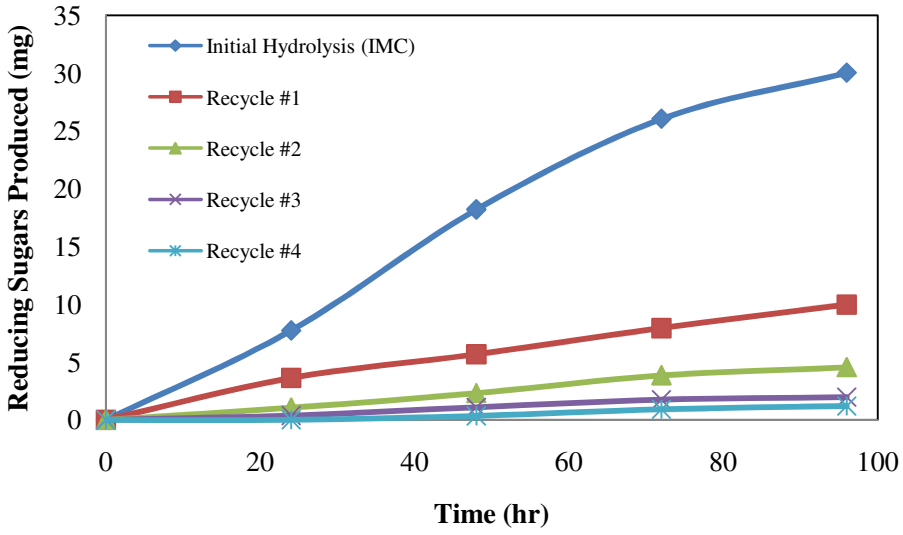

Figure 6.1: Reducing sugars produced over 4 recycles of cellulase immobilized on 100 mg of polystyrene-coated particles (1-2 µm).

A resulting loss in activity was demonstrated for the immobilized enzyme complex following each recycle. Activity was calculated after 96 hours of hydrolysis and is shown in Table 6.1 along with corresponding values for reducing sugars. The activity of immobilized

enzyme was determined to be 26.5% of the free enzyme activity following the initial hydrolysis reaction. Figure 6.2 displays the retention of enzymatic activity over time for each recycle. The overall activity loss following each recycle could have occurred as a result of various factors, which might include protein denaturation, end-product inhibition, loss of one or more individual components of the cellulase complex, and/or modification of an individual enzymes structure due to carbodiimide activation and immobilization on the support surface, to name a few.

Table 6.1: Activity and reducing sugar production for polystyrene-coated particles over 4 recycles of cellulose hydrolysis.

Recycle #	Hydrolysis Time (days)	Reducing Sugars Produced (mg)	Activity (μmol/mg-hr)	Activity Retained (%)
0	4	30.03	0.914	100.0
1	8	9.97	0.303	33.20
2	12	4.56	0.139	15.18
3	16	1.97	0.060	6.56
4	20	1.18	0.036	3.93

The overall efficiency of the cellulase complex immobilized on polystyrene-coated microparticles was also evaluated by comparing the total reducing sugars produced over 4 recycles to that produced by free enzyme of the same concentration (Figure 6.3). After 24 hours of hydrolysis, the total sugars produced equated to only 43% of the sugars produced by free enzyme. The immobilized enzyme complex remained relatively stable throughout the 96 hour reactions, at which point 42% of the free enzyme sugars were produced. This demonstrates that immobilization of the cellulase complex on polystyrene-coated particles produced similar results over 4 recycles as that of the free enzyme but at a lower level of efficiency.

It was hypothesized that the resulting loss in activity may be due, in part, to detachment of cellulase enzymes from the solid support. To support this theory the enzyme concentration in the supernatant (measured as protein) was measured following each reaction. The protein assay

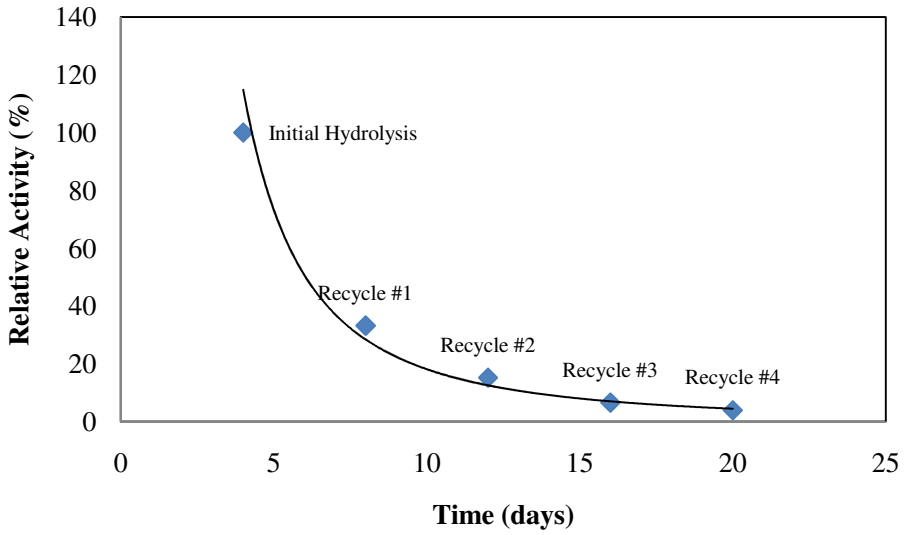

Figure 6.2: Activity retained for polystyrene-coated particles following each recycle.

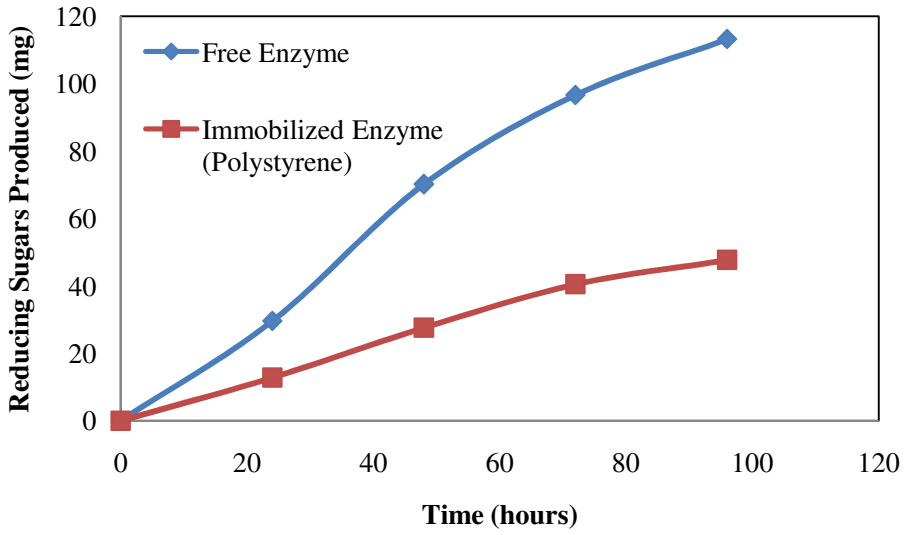

Figure 6.3: Comparison of total reducing sugars produced by the cellulase enzyme complex immobilized on polystyrene-coated particles over 4 recycles to that of free enzyme.

revealed a total loss of 30.2% of enzyme following the first recycle. The original attachment was 1.9 mg of protein giving a weight ratio of 0.019. An overall loss in enzyme and effect on reducing sugar production is displayed in Table 6.2. It is suggested that the initial loss was due to weakly bound enzyme becoming detached upon contact with the cellulosic substrate and, as a result, may have contributed to the steep loss in activity shown in Figure 6.2 following the initial hydrolysis and first recycle. It is likely that only a portion of the enzyme solution had effectively become covalently bound as a result of the carbodiimide reaction. Additional enzyme may have simply become adsorbed on the support surface allowing for easy detachment when subjected to the hydrolysis reaction. This could account for the high level of weakly bound enzyme becoming detached following the initial reaction.

An alternative suggestion for overall enzyme detachment can be attributed to shearing effects between individual particles during mixing and separation, resulting in a greater loss of enzyme. The loss due to shearing, however, was considered to be much less significant as compared to enzyme desorption, due to the reaction solution progressing under very gentle shaking. The resulting activity was corrected for enzyme loss and is shown in Figure 6.4, which demonstrates only a slight improvement over the original activity and suggests that the overall loss in activity was likely due to other factors, which were stated previously.

Table 6.2: Total enzyme released from polystyrene-coated particles and total sugar production corresponding to detachment.

Recycle #	Enzyme Released (%)	Remaining Enzyme Attached (%)	Total Reducing Sugars Produced (mg)	Reducing Sugars per Remaining Enzyme (mg/mg)
0	15.172	84.828	30.027	18.630
1	30.245	69.755	9.973	7.525
2	36.842	63.158	4.555	3.796
3	50.589	49.411	1.965	2.094
4	58.392	41.608	1.182	1.495

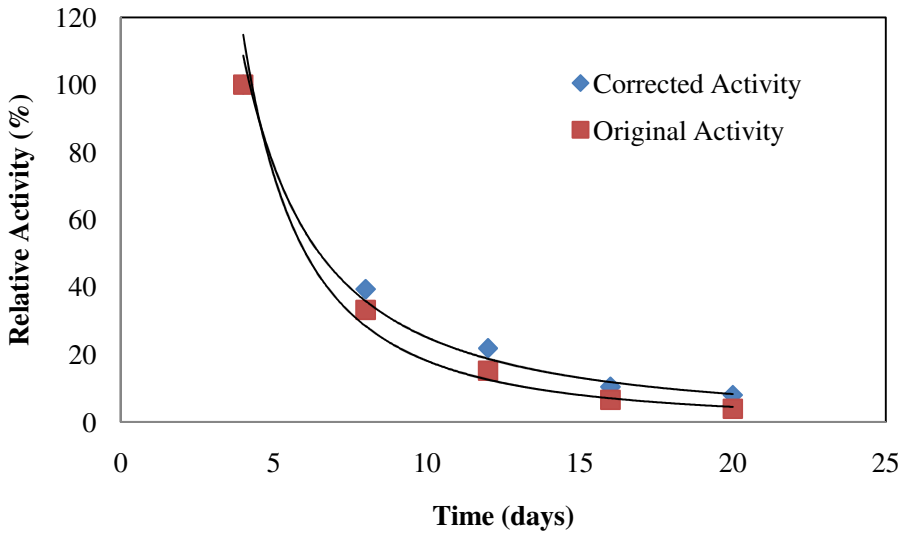

Figure 6.4: Corrected activity plot for immobilized cellulase as a result of enzyme detachment over 4 recycles during cellulose hydrolysis.

6.1.2 Comparison of Polystyrene-coated Particles to Fe_3O_4 Nanoparticles

When noting the efficiencies of enzyme-bound particles one must first take into consideration the size and surface areas for binding and the resultant activity. Fe_3O_4 nanopaticles had an average diameter of 13 nm, which is considerably smaller than the average diameter of polystyrene-coated magnetite particles of 1.5 µm. The major advantage for the nanoparticles is total surface area. The specific surface area (SSA) for the nanoparticles is 241660.9 mm^2/mm^3, which is 115 times larger than that of the polystyrene particles with an SSA of 2094.4 mm^2/mm^3. An increase in mass of 1992% for the microparticles would be required to have an equivalent surface area. The presence of a greater surface area allows for more efficient binding of the cellulase enzyme complex. A wider dispersion of binding occurs giving rise to higher activity retention; and, with minimal agglomeration, steric hindrance is less prevalent.

The complexity of the polymeric magnetite particles was evaluated and it was determined that polystyrene was much more prevalent, composing 96.2% of the polystyrene-iron oxide composite. A higher composition of polystyrene decreases the total mass, allowing the particles

to become more mobile in aqueous solution. This is demonstrated by comparing the densities of the iron oxide nanoparticles (5.18 g/cm^3) and the polymer-coated particles (0.939 g/cm^3). The performance of the cellulase enzyme complex was also compared for each particle type to determine if the material composition had any effects on enzymatic activity. This is demonstrated in Table 6.3. At first glance, the iron oxide nanoparticles appear to display greater performance over the polystyrene-coated particles; however, comparing the activity values for polymeric and iron oxide particles as a function of surface area verifies an overall increase in activity for polystyrene particles over the smaller nanoparticles. Activity retention also increased following each recycle reaching 20.6% after the 4th recycle. One possible reason for the changes in activity levels might be due to interactions between the support materials which may or may not have detrimental effects on the enzymes performance.

Table 6.3: Comparison of activity values as a function of surface area for Fe_3O_4 nanoparticles and polystyrene-coated microparticles.

	Activity (μmol/mg-hr)		**Activity per unit Surface Area**	
Recycle #	**Polystyrene**	**Fe_3O_4**	**Polystyrene**	**Fe_3O_4**
0	0.914	1.010	4.10E-06	1.80E-07
1	0.303	0.530	1.36E-06	9.47E-08
2	0.139	0.304	6.22E-07	5.43E-08
3	0.060	0.235	2.69E-07	4.20E-08
4	0.036	0.186	1.61E-07	3.32E-08
5	n/a	0.120	n/a	2.14E-08
6	n/a	0.111	n/a	1.98E-08

6.2 Conclusions

Cellulase enzyme complex was effectively immobilized on magnetic microparticles containing a polystyrene coating via carbodiimide activation and analyzed for recyclability. The enzyme-bound particles were successfully recycled over four trials after which the activity had

fallen to 4% of its original. The enzyme-to-support ratio was set at 0.019. Enzymatic activity was determined by measuring glucose as reducing sugars using the DNS colorimetric method. A minimal portion of the loss in activity was attributed to enzyme detachment from the solid support. This was verified by a protein assay conducted on the supernatant solution. Comparable to the Fe_3O_4 nanoparticles, it is suggested that a portion of enzyme had become adsorbed on the support surface as opposed to covalently binding, which allowed for easy detachment within the hydrolysis environment. The majority of activity, however, could have been lost as a result of several factors, which might include protein denaturation, end-product inhibition, loss of one or more individual components of the enzyme complex, and/or modification of the enzyme structure as a result of immobilization. The specific surface areas were calculated to compare the performance of nanoparticles over microparticles. A specific surface area of 241660.9 mm^2/mm^3 for the nanoparticles was 115 times greater in magnitude compared to the microparticles with a specific surface area of 2094.4 mm^2/mm^3. The larger surface area allowed for an even distribution of enzyme binding across the nanoparticle surface. The polymeric microparticles displayed higher activity retention when calculated as a function of surface area, which could have resulted from more amicable interactions between the cellulase enzyme complex and the polystyrene support surface.

7 CONCLUSIONS AND FUTURE RECOMMENDATIONS

7.1 Conclusions

The purpose of this study was to employ a practical method for recovery of a cellulase enzyme complex using magnetic particles. Fe_3O_4 nanoparticles were co-precipitated using Fe^{2+} and Fe^{3+} ions in conjunction with ammonium hydroxide. The enzyme complex was immobilized by carbodiimide activation of the enzymes carboxyl groups which were then covalently bound to amine functional groups on the nanoparticle surface. These particles were characterized using transmission electron microscopy (TEM) and were determined to have an average diameter of 13.3 nm. Immobilization of the enzyme did not cause any significant alteration in size or structure of the particles, nor did it cause any additional agglomeration. A Bradford protein assay was used to determine overall binding of the cellulase enzyme to the nanoparticles, and binding was confirmed using Fourier transform infrared (FTIR) spectroscopy and X-ray photoelectron spectroscopy (XPS).

Upon successful completion of the binding procedure, the enzyme-bound nanoparticles were introduced on to fresh cellulosic substrate at 50˚C and pH 5.0 for the hydrolysis reaction to ensue. The particles were recovered using a strong permanent magnet and recycled over a total of 6 trials before the enzymatic activity had fallen to 10% of its original. Evaluation of the overall performance of the immobilized cellulase complex over 6 recycles demonstrated that they only produced 76.8% of the overall sugars produced by free enzyme, indicating that the immobilization procedure was less effective overall. Activity was determined by measuring the glucose concentration produced as reducing sugars using the DNS colorimetric method. Sugar production was confirmed using high performance liquid chromatography (HPLC). The resultant loss in activity following each recycle was, in part, attributed to enzyme detachment from the solid support as determined by a protein assay of the supernatant. A total of 25% of the

original enzyme was lost following the initial reaction, and 64.5% was lost after the 6th recycle. The majority of activity loss, however, was likely due to other factors. Thermal stability was evaluated by measuring the reduction in activity over time during a single hydrolysis reaction. The free enzyme activity was reduced by approximately 49% after 72 hours of hydrolysis while the immobilized enzyme demonstrated a slight advantage in stability with an overall loss in activity of only 42%.

Characterization of the magnetite nanoparticles was conducted for determination of ideal parameters with which optimum sugar production could be achieved. Optimum binding efficiency for the cellulase enzyme complex was determined to occur at low enzyme loadings at which more than 90% of enzyme could be bound. Optimization of the enzyme-to-support weight ratio was an important factor in assessing the immobilized enzymes activity. The saturation point was determined to be 0.02. A higher loading of enzyme on the nanoparticle surface would cause a steric hindrance between individual cellulase molecules competing for substrate adsorption. Ionic forces between the enzyme complex and support surface can cause a change in the overall charge of the immobilized enzyme. This is verified by a noticeable shift in pH to 5.0 from the original pH of 4.0, which is ideal for the free enzyme. The optimum temperature was determined to be 50˚C for both the free and immobilized enzyme. An increase in thermal stability, however, allows the immobilized enzyme to be more durable over a broader range of temperatures.

With comparison to the enzyme-bound Fe_3O_4 nanoparticles, the cellulase enzyme was also immobilized on to magnetic particles coated with polystyrene and having a Fe_3O_4 core. The particles ranged in size from 1-2 μm and were successfully bound to the cellulase enzyme via carbodiimide activation. They were introduced to microcrystalline cellulosic substrate and were

effectively recovered and recycled over a total of 4 trials after which the resultant activity had fallen to approximately 4%. Further evaluation of the sugars produced over all 4 recycles revealed only 42% efficiency as compared to the sugar production by free enzyme. As with the magnetite nanoparticles, the resulting loss in activity following each trial was also, in part, attributed to protein detachment from the solid support. However, this provided only slight modification as the majority of activity loss was due to other factors, as was also demonstrated with the nanoparticles.

A major difference in the two particle variations is the overall size. The much smaller nanoparticles have a great advantage over the microparticle counterparts in that their specific surface area is roughly 115 times larger. This allows for a larger enzyme loading with less steric hindrance between molecules. The polystyrene microparticles did display an advantage in overall activity, however, when each particles activity was expressed as a function of unit surface area. This could be attributed to different interactions between the enzyme complex and particle surfaces.

In summary, enzyme immobilization has been demonstrated to have practical advantages for enzyme recovery and recycling which can lead to lower costs for ethanol fuels. Varying immobilization supports offer multiple advantages and disadvantages, but magnetic particles possess tremendous potential, especially when coupled with polymers. As stated in previous research[47, 82], a polymeric spacer could also be employed and has demonstrated positive results for retaining enzyme activity. Ideally, the nanoparticles would be bound to a ligand spacer prior to enzyme immobilization. This would allow the advantages of a magnetic core with high surface area in addition to a spacer arm giving the enzyme molecules more freedom of motion and allowing more active sites to remain available for substrate adsorption. Optimization of this

procedure would garner many benefits, not only with biofuels, but with biological, biomedical, and environmental applications; these might include more efficient site-specific drug delivery, separation and purification of biological molecules and cells, and development of biosensors for measuring low concentrations of bacteria and protein detection.

7.2 Future Recommendations

When paramagnetic nanoparticles are dispersed in microfluid, the permanent magnetization is evenly distributed throughout the fluid and hence gets compensated. As a result, particle agglomeration is prevented. As particle size increases, magnetic interactions between particles predominate leading to particle aggregation[83]. A further study to decrease the degree of aggregation would be a worthwhile endeavor. One possible solution would be to introduce surfactants to coat the particles during synthesis. Some notable surfactants may include oleic acid[84] or zirconia[85]. Additionally, aggregation tends to increase over time with nanoparticles in solution, and also with drying or centrifugation of the particles. Therefore, the use of freshly prepared nanoparticles that remain in aqueous solution throughout would be an ideal practice.

Additional optimization may be achieved by covalent attachment of a polymeric spacer on the surface of the magnetic Fe_3O_4 nanoparticles. Although the synthesis may be fairly complicated, it would allow increased binding and enzyme utilization by maximizing surface area. Varying polymers should be researched to optimize compatibility with the cellulase enzymes. Some polymers which have shown varying degrees of potential include polyvinyl alcohol (PVA) or polyethylene glycol (PEG)[47], and sepharose/agarose[82]. Moreover, it may also be worthwhile to explore alternative forms for covalent attachment. Other notable methods include the use of silane coupling agents and the gluteraldehyde method which has previously shown favorable results over carbodiimide activation[4, 47].

A separate concern which arose during the present study involved the detachment of cellulase enzyme from the particle surface. This may be due to weakly bound enzyme that was initially adsorbed on the support surface instead of covalent binding; however, it may also be contributed by shearing forces resulting from particle contact during stirring or shaking of the reaction solution. Pinpointing the exact causes of this effect may also prove sufficient for this research. One possible alternative may be to immobilize the enzyme on a grating within a packed-bed reactor. However, the shearing forces produced by the influx flow of substrate within the vessel would have to be addressed as well. A separate alternative may be to encapsulate the enzyme within a matrix. This would require a pore size large enough to permit the cellulosic substrate to come in contact with the immobilized enzyme.

The sheer size of the nanoparticles should also be considered when measuring recyclability. At the nano-scale these particles will remain in suspension for much longer periods of time. When recovering these particles via a magnetic field, it is likely that some will be removed from the solution during washing steps. Therefore, it would also be worthwhile to determine the recovery efficiency of the nanoparticles over multiple hydrolysis trials.

Lastly, characterization of the magnetite nanoparticles is performed using transmission electron microscopy (TEM). Additional analysis should also be explored to obtain a more practical method for size determination which would also account for aggregation. Some noteworthy alternatives include atomic force microscopy (AFM)[86], asymmetrical flow field-flow-fractionation (A4F)[86-88], and magnetic field-flow-fractionation (MFFF)[89], all of which have demonstrated favorable results for characterization of particles at the nano-scale.

REFERENCES

1. Pimentel, D. and M.H. Pimentel, *Food, Energy, and Society*. 3 ed. 2007: CRC Press. 380.

2. Perlack, R.D., et al., *Biomass as Feedstock for a Bioenergy and Bioproducts Industry: The Technical Feasibility of a Billion-Ton Annual Supply*. 2005, US Department of Energy, US Department of Agriculture, Oak Ridge National Laboratory: Oak Ridge, Tennessee.

3. Badger, P.C., *Ethanol From Cellulose: A General Review*. Trends in new crops and new uses., ed. Jules Jannick and A. Whipkey. Vol. 5. 2002, Alexandria, VA: ASHS Press. 17-21.

4. Oh, S., *Enzymatic Hydrolysis of Cellulosic Biomass by Using Immobilized Cellulase*, in *Chemical Engineering*. 1982, Texas Tech University: Dallas, TX.

5. Robertis, E.D.P.D., W.W. Nowinski, and F.A. Saez, *Cell Biology*. 5 ed. 1970, Philadelphia: W.B. Saunders. 178.

6. Ghose, T.K., *Measurement of Cellulase Activities.* International Union of Pure and Applied Chemistry, 1987. **59**(2): p. 257-268.

7. Mansfield, S.D. and R. Meder, *Cellulose hydrolysis - the role of monocomponent cellulases in crystalline cellulose degradation.* Cellulose, 2003. **10**: p. 159-169.

8. Imai, M., K. Ikari, and I. Suzuki, *High-performance hydrolysis of cellulose using mixed cellulase species and ultrasoncation pretreatment.* Biochemical Engineering, 2004. **17**: p. 79-83.

9. Atalla, R.H. *The Structures of Native Celluloses*. in *Foundation for Biotechnical and Industrial Fermentation Research*. 1993. Espoo, Finland.

10. Chernaglazov, V.M., O.V. Ermolova, and A.A. Klyosov, *Adsorption of high perity endo-1-4-B-glucanases from Trichoderma reesei on components of lignocellulosic materials: cellulose, lignin, and xylan.* Enzyme and Microbial Technology, 1988. **10**: p. 503-507.

11. Ooshima, H., D.S. Burns, and A.O. Converse, *Adsorption of cellulase from Trichoderma reesei on cellulose and lignacious residue in wood pretreated by dilute sulfuric acid with explosive decompression.* Biotechnology and Bioengineering, 1990. **36**(5): p. 446-452.

12. Girard, D.J. and A.O. Converse, *Recovery of cellulase from lignaceous hydrolysis residue* Applied Biochemistry and Biotechnology, 1993. **39-40**(1): p. 521-533.

13. Tanaka, M., et al., *Saccharification of cellulose by combined hydrolysis with acid and enzyme.* Journal of Fermentation Technology, 1980. **58**: p. 517.

14. Lee, D., A.H.C. Yu, and J.N. Saddler, *Evaluation of Cellulase Recycling Strategies for the Hydrolysis of Lignocellulosic Substrates.* Biotechnology and Bioengineering, 1995. **45**(4): p. 328-336.

15. Gregg, D.J. and J.N. Saddler, *Factors affecting cellulose hydrolysis and the potential of enzyme recycle to enhance the efficiency of an integrated wood to ethanol process.* Biotechnology and Bioengineering, 1996. **51**(4): p. 375 - 383.

16. Lu, Y., et al., *Cellulase Adsorption and and Evaluation of Enzyme Recycle During Hydrolysis of Steam-Exploded Softwood Residues.* Applied Biochemistry and Biotechnology, 2002. **98-100**(1-9): p. 641-654.

17. Martína, C., H.B. Klinkea, and A.B. Thomsena, *Wet oxidation as a pretreatment method for enhancing the enzymatic convertibility of sugarcane bagasse.* Enzyme and Microbial Technology, 2007. **40**(3): p. 426-432.

18. Meunier-Goddik, L. and M.H. Penner, *Enzyme-Catalyzed Saccharification of Model Celluloses in the Presence of Lignacious Residues* J. Agric. Food Chem., 1999. **47**(1): p. 346 -351.

19. Ryu, D.D.Y., et al., *Effect of compression milling on cellulose structure and on enzymatic hydrolysis kinetics.* Biotechnology and Bioengineering, 1982. **24**(5): p. 1047 - 1067.

20. Ryu, D.D.Y., C. Kim, and M. Mandels, *Competitive Adsorption of Cellulase Components and its Significance in A Synergistic Mechanism.* Biotechnology and Bioengineering, 1984. **26**: p. 488-496.

21. Henrissat, B., et al., *Synergism of Cellulases from Trichoderma reesei in the Degradation of Cellulose.* Bio/Technology, 1985. **3**: p. 722-726.

22. Okada, G., *Purification and Properties of a Cellulase from Aspergillus niger.* Agricultural and Biological Chemistry, 1985. **49**(5): p. 1257-1265.

23. Shen, Y., L.M. Wang, and K. Sun, *Kinetics of the Cellulase Catalyzed Hydrolysis of Cellulose Fibers.* Journal of Textile Research, 2004. **74**(6): p. 539-545.

24. Almeida, L. and A. Cavaco-Paulo, *Softening of Cotton by Enzymatic Hydrolysis.* Melliand Textilberichte, 1993. **74**: p. 404-407.

25. Sridsodsuk, M., et al., *Modes of action on cotton and bacterial cellulose of a homologous endoglucanase-exoglucanase pair from Trichoderma reesei.* European Journal of Biochemistry, 1998. **251**: p. 885-892.

26. Sasaki, T., et al., *Correlation between X-ray diffraction measurements of cellulose crystalline and the susceptibility to microbial cellulase.* Biotechnology and Bioengineering, 1979. **21**: p. 1031-1042.

27. Fagerstam, L.G. and L.G. Pettersson, *The 1,4-B-D-glucan cellobiohydrolases of Trichoderma reesei QM 9414. A new type of cellulolytic synergism.* FEBS Letters, 1980. **119**: p. 97-100.

28. Chanzy, H., et al., *The action of 1,4-B-glucan cellobiohydrolase on Valonia cellulose microcrystals. An electron microscopy study.* FEBS Letters, 1983. **153**: p. 113-118.

29. Sternberg, D., *Beta-Glucosidase of Trichoderma: Its Biosynthesis and Role in Saccharification of Cellulose.* Applied and Environmental Microbiology, 1976. **31**(5): p. 648-654.

30. Sternberg, D., P. Vijayakumar, and E.T. Reese, *Beta-Glucosidase: microbial production and effect on enzymatic hydrolysis of cellulose.* Canadian Journal of Microbiology, 1977. **23**(2): p. 139-147.

31. Deschamps, F. and M.C. Huet, *Xylanase production in solid-state fermentation: a study of its properties.* Applied Microbiology and Biotechnology, 1985. **22**: p. 177-180.

32. Brown, L. and R. Torget, *Enzymatic Saccharification of Lignocellulosic Biomass*, in *Laboratory Analytical Procedure (LAP-009)*. 1996, NREL. p. 1-8.

33. McDougall, J., *A hydro-bio-mechanical model for settlement and other behavior in land filled waste.* Computers and Geotechnics, 2007. **34**: p. 229-246.

34. Peiris, P.S. and I. Silva, *Hydrolysis of rice straw to fermentable sugars by Trichoderma enzymes.* MIRCEN Journal, 1987. **3**: p. 57-65.

35. Herr, D., *Conversion of Cellulose to Glucose with Cellulase of Trichoderma viride ITCC-1433.* Biotechnology and Bioengineering, 1980. **22**: p. 1601-1612.

36. Sun, Y. and J. Cheng, *Enzymatic Hydrolysis of Rye Straw and Bermuda Grass Using Cellulases Supplemented with B-glucosidases.* Transactions of the ASAE, 2004. **47**(1): p. 343-349.

37. Tjerneld, F., I. Persson, and J.M. Lee, *Enzymatic Cellulose Hydrolysis in an Attrition Bioreactor Combined with an Aqueous Two-Phase System.* Biotechnology and Bioengineering, 1991. **37**: p. 876-882.

38. Karube, I., et al., *Hydrolysis of Cellulose in a Cellulase-Bead Fluidized Bed Reactor.* Biotechnology and Bioengineering, 1977. **19**: p. 1183-1191.

39. McAloon, A., et al., *Determining the Cost of Producing Ethanol from Corn Starch and Lignocellulosic Feedstocks*, in *Technical Report*. 2000, NREL, USDA, USDOE: Golden, Colorado. p. 1-30.

40. Ramos, L.P., C. Breuil, and J.N. Saddler, *The use of enzyme recycling and the influence of sugar accumulation on cellulose hydrolysis by Trichoderma cellulases.* Enzyme and Microbial Technology, 1993. **15**: p. 19-25.

41. Ohlson, I. and G. Tragardh, *Enzymatic Hydrolysis of Sodium-Hydroxide-Pretreated Sallow in an Ultrafiltration Membrane Reactor.* Biotechnology and Bioengineering, 1984. **26**: p. 647-653.

42. Mores, W.D., J.S. Knutsen, and R.H. Davis, *Cellulase Recovery via Membrane Filtration.* Applied Biochemistry and Biotechnology, 2001. **91-93**: p. 297-309.

43. Gan, Q., S.J. Allen, and G. Taylor, *Design and operation of an integrated membrane reactor for enzymatic cellulose hydrolysis.* Biochemical Engineering Journal, 2002. **12**: p. 223-229.

44. Hahn-Hagerdal, B., *An Enzyme Coimmobilized with a Microorganism: The Conversion of Cellobiose to Ethanol using B-glucosidase and Saccharomyces cerevisiae in Calcium Alginate Gels.* Biotechnology and Bioengineering, 1984. **26**: p. 771-774.

45. Brockman, H.L., J.H. Law, and F.J. Kezdy, *Catalysis by Adsorbed Enzymes. The Hydrolysis of Tripropionin by Pancreatic Lipase Adsorbed to Siliconized Glass Beads.* Journal of Biological Chemistry, 1973. **248**(14): p. 4965-4970.

46. Wang, P., et al., *Enzyme Stabilization by Covalent Binding in Nanoporous Sol-Gel Glass for Nonaqueous Biocatalysis.* Biotechnology and Bioengineering, 2001. **74**(3): p. 249-255.

47. Garcia III, A., S. Oh, and C.R. Engler, *Cellulase Immobilization on Fe_3O_4 and Characterization.* Biotechnology and Bioengineering, 1989. **33**: p. 321-326.

48. Stratulat, R., G. Calugaru, and V. Badescu, *Magnetic Carriers Particles for Selective Separation in Environmental and Industrial Processes.* Anlele Stiintifice Ale Universitatii "AL.I.CUZA" IASI, 2000: p. 45-50.

49. Chen, D.-H. and M.-H. Liao, *Preparation and characterization of YADH-bound magnetic nanoparticles.* Journal of Molecular Catalysis B: Enzymatic, 2002. **16**: p. 283-291.

50. Kouassi, G.K., J. Irudayaraj, and G. McCarty, *Activity of glucose oxidase functionalized onto magnetic nanoparticles.* BioMagnetic Research and Technology, 2005. **3**(1).

51. Johnson, A.K., et al., *Novel method for immobilization of enzymes to magnetic nanoparticles.* Journal of Nanoparticle Research, 2007.

52. Sharma, A., et al., *Dramatic Increase in Stability and Longevity of Enzymes Attached to Monodispersive Iron Nanoparticles.* IEEE Transactions on Magnetics, 2007. **43**(6): p. 2418-2420.

53. Zhang, Y., N. Kohler, and M. Zhang, *Surface modification of superparamagnetic magnetite nanoparticles and their intracellular uptake.* BioMaterials, 2002. **23**: p. 1553-1561.

54. Petri-Fink, A., et al., *Development of functionalized superparamagnetic iron oxide nanoparticles for interaction with human cancer cells.* BioMaterials, 2005. **26**: p. 2685-2694.

55. Holzapfel, V., et al., *Synthesis and biomedical applications of functionalized fluorescent and magnetic dual reporter nanoparticles as obtained in the miniemulsion process.* Journal of Physics: Condensed Matter, 2006. **18**: p. S2581-S2594.

56. Dincer, A. and A. Telefoncu, *Improving the stability of cellulase by immobilization on modified polyvinyl alcohol coated chitosan beads.* Journal of Molecular Catalysis B: Enzymatic, 2007. **45**: p. 10-14.

57. Garcia, I., et al., *Generation of Core/Shell Iron Oxide Magnetic Nanoparticles with Polystyrene Brushes by Atom Transfer Radical Polymerization.* Journal of Polymer Science: Part A: Polymer Chemistry, 2007. **45**: p. 4744-4750.

58. Kim, Y.H., et al., *Coating of magnetic particle with polystyrene and its magnetorheological characterization.* Physica Status Solidi, 2007. **204**(12): p. 4178-4181.

59. Yang, C., et al., *Surface Functionalization and Characterization of Magnetic Polystyrene Microbeads.* Langmuir, 2008. **24**(16): p. 9006-9010.

60. Zang, F., et al., *Synthesis and Characterization of Polystyrene-Grafted Magnetite Nanoparticles.* Collois Polymer Science, 2008. **286**: p. 837-841.

61. Bornscheuer, U.T., *Immobilizing Enzymes: How to Create More Suitable Biocatalysts.* Angewandte Chemie International Edition, 2003. **42**(29): p. 3336-3337.

62. Ghose, T.K. and V.S. Bisaria, *Studies on the mechanism of enzymatic hydrolysis of cellulosic substances.* Biotechnology and Bioengineering, 1979. **21**(1): p. 131-146.

63. Gilbert, I.G. and G.T. Tsao, *Interaction between solid substrate and cellulase enzymes in cellulose hydrolysis.* Annual Reports on Fermentation Processes (USA), 1983. **6**: p. 323-358.

64. Takimoto, A., et al., *Encapsulation of cellulase with mesoporous silica (SBA-15).* Microporous and Mesoporous Materials, 2008. **116**: p. 601-606.

65. Ge, Y., et al., *Co-immobilization of cellulase and glucose isomerase by molecular deposition technique.* Biotechnology Techniques, 1997. **11**(5): p. 359-361.

66. Feng, T., et al., *Immobilization of a Nonspecific Chitosan Hydrolytic Enzyme for Application in Preparation of Water-Soluble Low-Molecular-Weight Chitosan.* Journal of Applied Polymer Science, 2006. **101**: p. 1334-1339.

67. Shinkai, M., H. Honda, and T. Kobayashi, *Preparation of Fine Magnetic Particles and Application for Enzyme Immobilization* Biocatalysis and Biotransformation, 1991. **5**(1): p. 61-69.

68. Gao, X., et al., *Colloidal stable silica encapsulated nano-magnetic composite as a novel bio-catalyst carrier.* Chemical Communications, 2003(24): p. 2998-2999.

69. West, J.L. and N.J. Halas, *Applications of nanotechnology to biotechnology - Commentary.* Current Opinion in Biotechnology, 2000. **11**(2): p. 215-217.

70. Curtis, A. and C. Wilkinson, *Nanotechniques and approaches in biotechnology.* Trends in Biotechnology, 2001. **19**(3): p. 97-101.

71. Tartaj, P., et al., *Advances in magnetic nanoparticles for biotechnology applications.* Journal of Magnetism and Magnetic Materials, 2005. **290-291**: p. 28-34.

72. Halling, P.J. and P. Dunnill, *Magnetic supports for immobilized enzymes and bioaffinity adsorbents.* Enzyme and Microbial Technology, 1980. **2**(1): p. 2-10.

73. Gupta, A.K. and M. Gupta, *Synthesis and surface engineering of iron oxide nanoparticles for biomedical applications.* BioMaterials, 2005. **26**(18): p. 3995-4021.

74. Ito, A., et al., *Medical Application of Functionalized Magnetic Nanoparticles.* Journal of Bioscience and Bioengineering, 2005. **100**(1): p. 1-11.

75. Mehta, R.V., et al., *Direct Binding of Proteins to Magnetic Particles.* Biotechnology Techniques,, 1997. **11**(7): p. 493-496.

76. Koneracka, M., et al., *Immobilization of proteins and enzymes to fine magnetic particles.* Journal of Magnetism and Magnetic Materials, 1999. **201**(1-3): p. 427-430.

77. Miller, G.L., *Use of Dinitrosaylicylic Acid Reagent for Determination of Reducing Sugar.* Analytical Chemistry, 1959. **31**(3): p. 426-428.

78. Bradford, M.M., *A Rapid and Sensitive Method for the Quantitation of Microgram Quantities of Protein Utilizing the Principle of Protein-Dye Binding.* Analytical Biochemistry, 1976. **72**: p. 248-254.

79. Goldstein, L., Y. Levin, and E. Katchalski, *A Water-Insoluble Polyanionic Derivative of Trypsin. II. Effect of the Polyelectrolyte Carrier on the Kinetic Behavior of the Bound Trypsin.* Biochemistry, 1964. **3**(12): p. 1913-1919.

80. Goldstein, L. and E. Katchalski, *Use of water-insoluble enzyme derivatives in biochemical analysis and separation.* Fresnius Z. Anal. Chem., 1968. **243**: p. 375-396.

81. Weetall, H., *Preparation of Immobilized Proteins Covalently Coupled Through Silane Coupling Agents to Inorganic Supports.* Applied Biochemistry and Biotechnology, 1993. **41**: p. 157-188.

82. Chim-anage, P., et al., *Properties of Cellulase Immobilized on Agarose Gel with Spacer.* Biotechnology and Bioengineering, 1986. **28**: p. 1876-1878.

83. Nidumolu, B.S.G.R., *Functionalization of Gold and Glass Surfaces with Magnetic Nanoparticles Using Biomolecular Interactions*, in *Biological & Agricultural Engineering*. 2005, Louisiana State University: Baton Rouge, LA.

84. Horak, D., N. Smenyuk, and F. Lednicky, *Effect of the Reaction Parameters on the Particle Size in the Dispersion Polymerization of 2-Hydroxyethyl and Glycidyl Methacrylate in the Presence of a Ferrofluid.* Journal of Polymer Science Part A: Polymer Chemistry, 2003. **41**(12): p. 1848-1863.

85. Han, S., et al., *Diameter-Controlled Synthesis of Discrete and Uniform-Sized Single-Walled Carbon Nanotubes Using Monodisperse Iron Oxide Nanoparticles Embedded in Zirconia Nanoparticle Arrays as Catalysts.* Journal Of Physical Chemistry B, 2004. **108**(24): p. 8091-8095.

86. Baalousha, M. and J.R. Lead, *Characterization of Natural Aquatic Colloids (< 5 nm) by Flow-Field-Flow Fractionation and Atomic Force Microscopy.* Environmental Science and Technology, 2007. **41**(4): p. 1111-1117.

87. Baalousha, M., et al., *Aggregation and Surface Properties of Iron Oxide Nanoparticles: Influence of pH and Natural Organic Matter.* Environmental Toxicology and Chemistry, 2008. **27**(9): p. 1875-1882.

88. Lohrke, J., A. Briel, and K. Maeder, *Characterization of Superparamagnetic Iron Oxide Nanoparticles by Asymmetrical Flow-Field-Flow Fractionation.* Nanomedicine, 2008. **3**(4): p. 437-452.

89. Latham, A.H., et al., *Capillary Magnetic Field Flow Fractionation and Analysis of Magnetic Nanoparticles.* Analytical Chemistry, 2005. **77**(15): p. 5055-5062.

APPENDIX A: RAW DATA AND STATISTICS FOR RECYCLING OF MAGNETITE NANOPARTICLES (SPION)

Table A.1: Reducing sugars produced over 6 recycles of cellulase-bound Fe_3O_4 nanoparticles.

	Time (hr)	24			48			72			96		
Recycle #	**Replicate #**	EB	SB	ES	EB	SB	ES	EB	SB	ES	EB	SB	ES
0	1	1.16	0.63	37.2	0.21	0.74	50.6	2	0.74	70.3	3.37	0.11	76.4
	2	1.47	0.84	30.9	0.11	0.53	58.7	2	0.74	61.5	1.79	0.21	75.1
	3	1.58	1.05	29.1	0.11	0.63	49.6	1.68	0.63	62.3	1.68	0.11	77.5
1	1	3.37	1.16	9.68	2.84	1.68	23.1	1.47	0	33.3	0.42	1.37	42.2
	2	2.95	1.16	6.84	2	1.47	20	1.37	0.11	29.3	0.53	1.79	39.1
	3	3.16	1.16	13.7	2.63	2.21	24.9	2	0.42	33.4	0.74	1.79	41.7
2	1	0.53	1.16	9.68	0.63	1.89	18.8	0.63	1.89	26	0.95	2.11	31.1
	2	0.63	1.26	10.1	0.84	1.89	20.5	1.16	2.21	27.7	1.58	2.42	32.2
	3	0.63	1.26	9.79	0.95	1.79	20.1	2	2.11	27.3	2.53	2.11	31.5
3	1	0.25	0.34	6.76	0.17	0	10.1	0.68	0	14.3	0.51	0	19.4
	2	0.59	0.42	5.24	0.08	0	7.86	0	0	12.7	0.68	0.17	16.9
	3	0.93	0.17	6.09	0.08	0	9.72	0	0	13.1	0.76	0.17	17.6
4	1	0	0	3.55	1.78	0.17	9.21	1.44	0.25	13.2	0.34	2.03	19.4
	2	0.34	0	4.14	2.2	0.17	7.95	0.85	0.34	10.8	0.68	1.94	15.7
	3	0	0	3.8	0.93	0.25	6.93	0.85	0.42	9.97	1.69	2.11	14.5
5	1	1.44	1.1	3.89	0.17	1.78	6.68	0.42	1.78	10.9	0.76	1.94	14.5
	2	1.35	1.1	2.79	0.51	1.69	5.07	0.68	1.69	8.03	1.35	2.11	11.2
	3	1.52	0.85	3.04	0.76	1.86	5.58	1.27	1.61	8.37	2.03	2.28	11.1
6	1	2.62	1.69	5.16	0.42	1.86	7.27	0.42	2.28	10.3	0.51	2.03	12.9
	2	2.03	1.52	3.47	0.34	1.94	5.07	0.68	2.28	7.52	0.93	2.11	9.55
	3	1.94	1.86	3.72	1.01	2.11	5.92	1.1	2.11	8.79	1.27	2.28	11

* EB = Enzyme Blank, SB = Substrate Blank, ES = Enzyme-Substrate Complex

Table A.2: Statistical analysis for reducing sugars produced by recycled nanoparticles.

Recycle #	Statistic	Time (hr)			
		24	48	72	96
0	Mean	30.140	52.211	62.105	73.895
	SD	4.251	5.013	4.884	1.539
	CV (%)	14.103	9.601	7.864	2.082
1	Mean	5.754	18.386	30.175	38.772
	SD	3.444	2.563	2.375	1.717
	CV (%)	59.846	13.938	7.870	4.428
2	Mean	8.035	17.158	23.649	27.684
	SD	0.235	0.893	1.127	1.004
	CV (%)	2.929	5.206	4.766	3.627
3	Mean	5.128	9.129	13.130	17.216
	SD	0.844	1.215	0.920	1.323
	CV (%)	16.456	13.311	7.003	7.685
4	Mean	3.719	6.199	9.946	13.609
	SD	0.355	1.314	1.702	2.609
	CV (%)	9.553	21.199	17.110	19.171
5	Mean	0.789	3.522	6.622	8.763
	SD	0.600	0.877	1.632	2.083
	CV (%)	76.014	24.903	24.644	23.772
6	Mean	0.225	3.522	5.917	8.115
	SD	0.998	1.175	1.441	1.744
	CV (%)	442.648	33.371	24.356	21.491

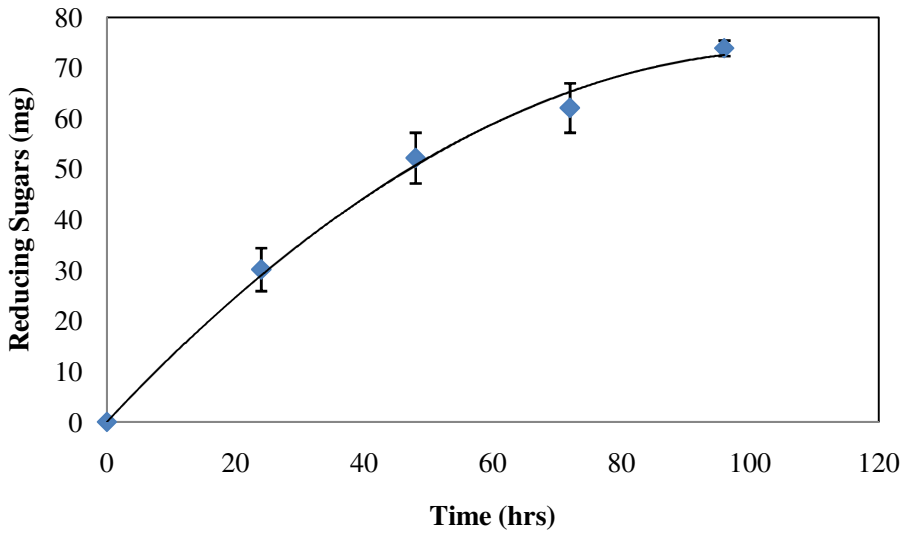

Figure A.1: Mean reducing sugar production for initial hydrolysis with cellulase-bound nanoparticles.

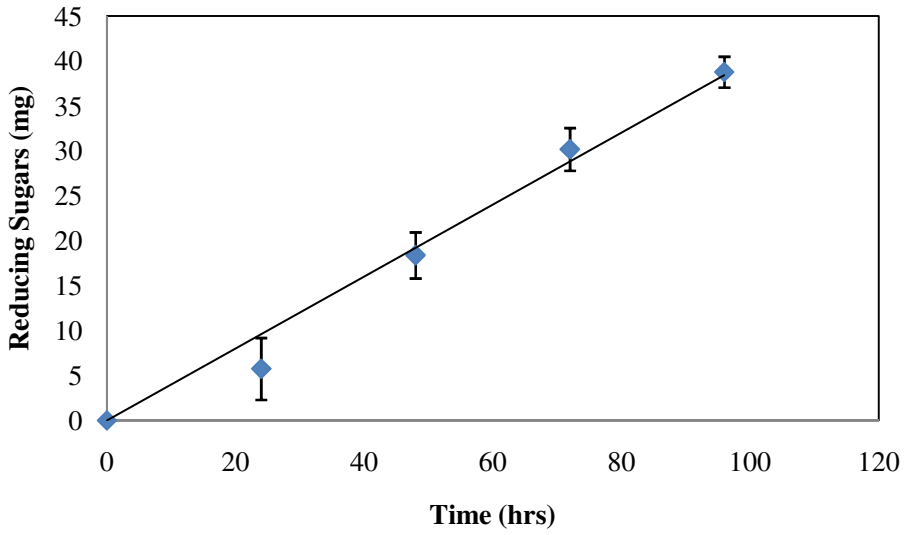

Figure A.2: Mean reducing sugar production for 1st recycle of cellulase-bound nanoparticles.

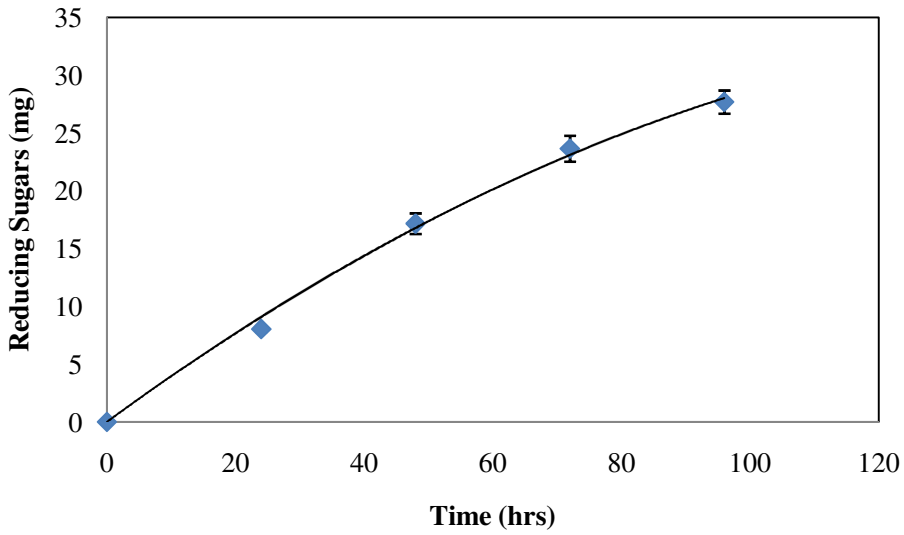

Figure A.3: Mean reducing sugar production for 2nd recycle of cellulase-bound nanoparticles.

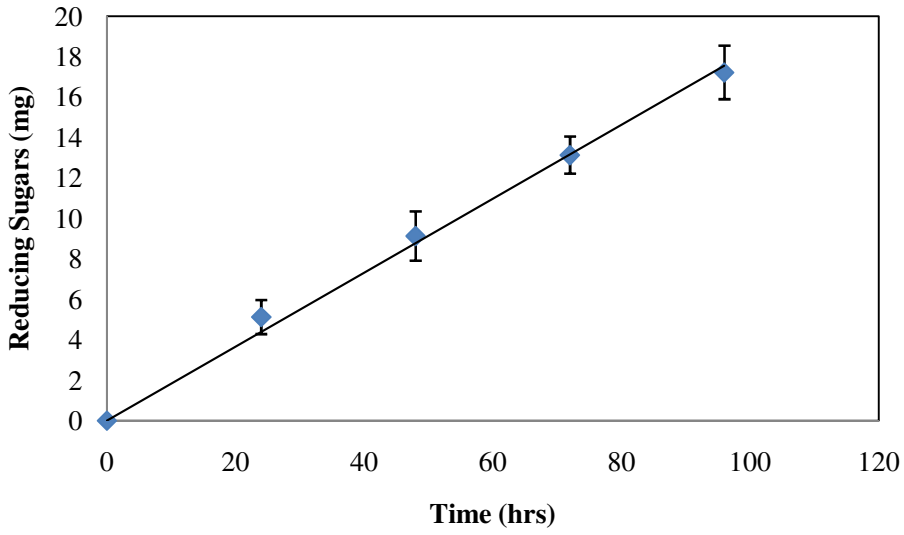

Figure A.4: Mean reducing sugar production for 3rd recycle of cellulase-bound nanoparticles.

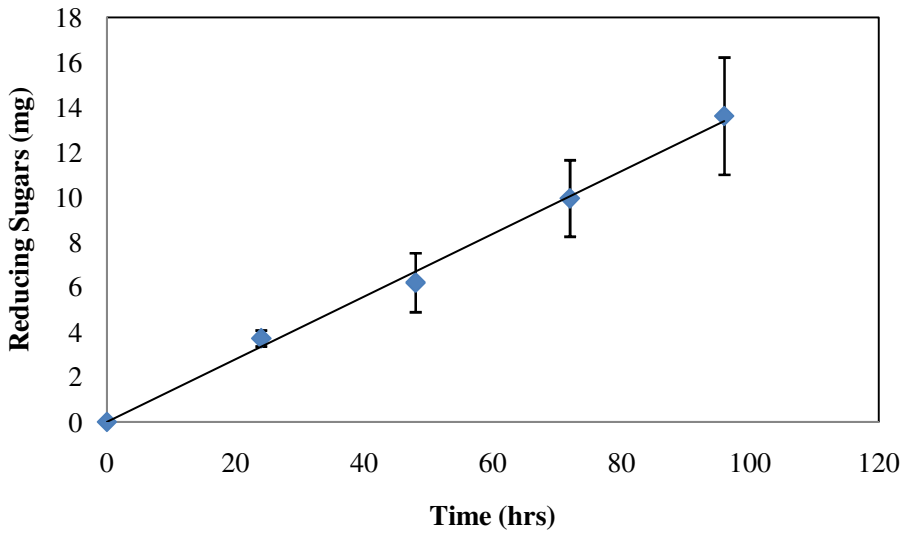

Figure A.5: Mean reducing sugar production for 4th recycle of cellulase-bound nanoparticles.

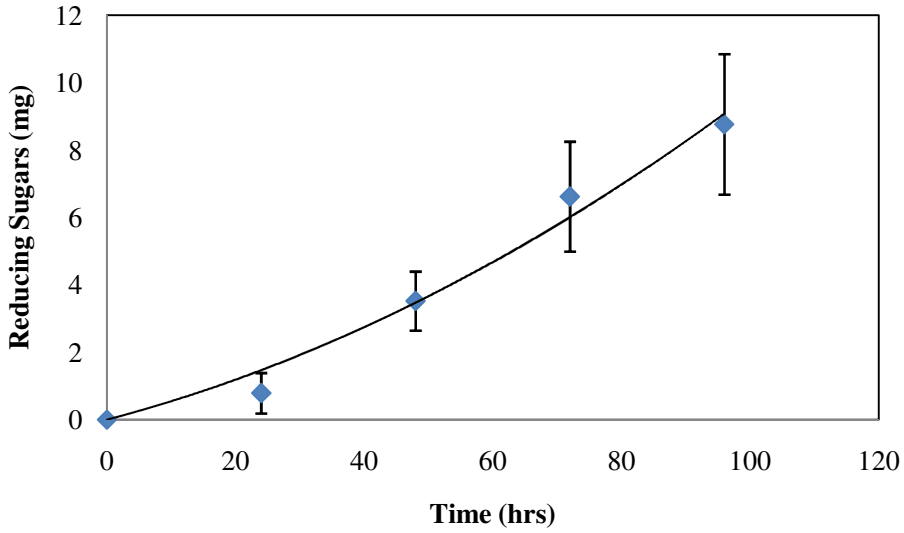

Figure A.6: Mean reducing sugar production for 5th recycle of cellulase-bound nanoparticles.

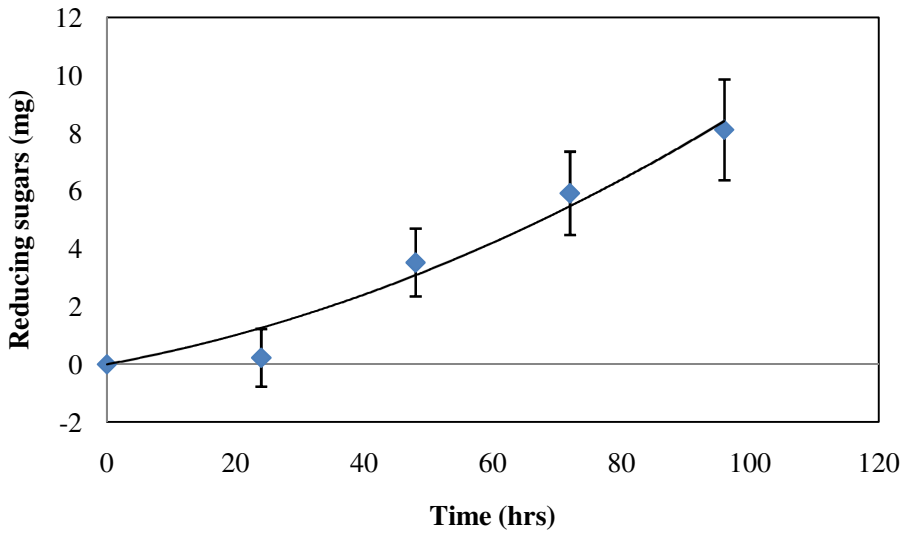

Figure A.7: Mean reducing sugar production for 6th recycle of cellulase-bound nanoparticles.

APPENDIX B: RAW DATA AND STATISTICS FOR CHARACTERIZATION AND OPTIMIZATION EXPERIMENTS

Table B.1: Binding efficiency for varying amounts of cellulase enzyme added to 50 mg of Fe_3O_4 nanoparticles and statistical analysis.

		Protein Added (mg)				
		1	3	6	12	18
Bound Protein (mg)	Replicate 1	0.7974487	1.0524208	1.3887261	1.9603517	2.7215997
	Replicate 2	0.9753188	1.3883176	1.335253	1.8362814	2.2657343
	Replicate 3	0.938297	1.151378	1.5376388	1.747429	1.9843686
Mean		0.904	1.197	1.421	1.848	2.324
Standard Deviation		0.094	0.173	0.105	0.107	0.372
CV (%)		10.385	14.416	7.383	5.787	16.009

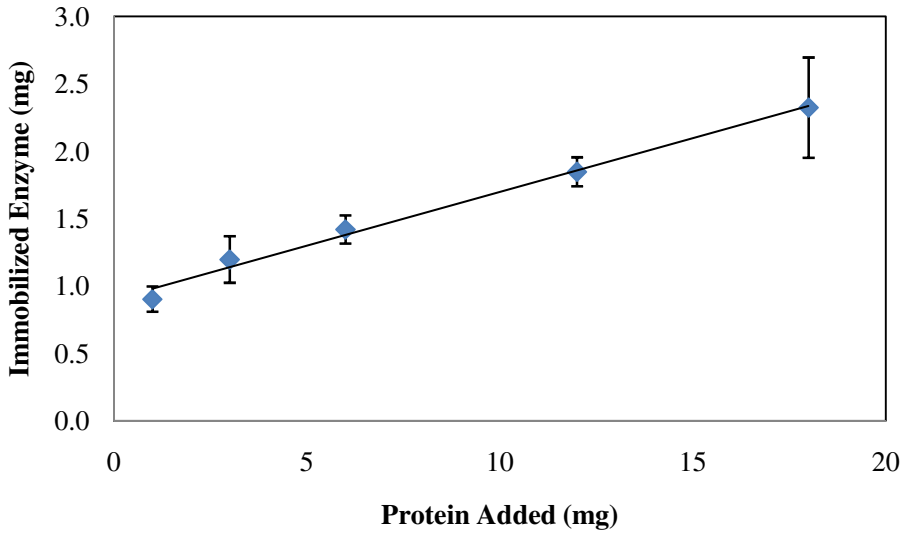

Figure B.1: Binding analysis for cellulase immobilized on 50 mg of Fe_3O_4 nanoparticles.

Table B.2: Effect of weight ratio on reducing sugar production and statistical analysis.

Weight Ratio (mg/mg)		0.01564			0.02084			0.02818		
		EB	SB	ES	EB	SB	ES	EB	SB	ES
Reducing Sugars (mg)	Replicate 1	0.0254	1.1031	1.6103	0.0063	1.1031	3.4045	0.1268	2.3394	3.0685
	Replicate 2	0.0571	1.1412	3.1382	0	1.1412	3.956	0.1395	1.0841	3.1128
	Replicate 3	0.0507	1.0904	1.5469	0.0127	1.0904	1.8829	0.1522	1.1285	2.9861
Activity (µmol/mg-hr)			40.140			62.747			33.067	
Mean			0.943			1.963			1.399	
Standard Deviation			0.902			1.074			0.715	
CV (%)			95.651			54.709			51.129	

Weight Ratio (mg/mg)		0.05444			0.08362			0.15946		
		EB	SB	ES	EB	SB	ES	EB	SB	ES
Reducing Sugars (mg)	Replicate 1	0.038	1.1031	3.7595	0.0761	1.1031	4.7422	0.1395	0.4903	5.2557
	Replicate 2	0.019	1.1412	3.1255	0.0697	1.1412	3.6771	0.1458	1.1412	3.9687
	Replicate 3	0.038	1.0904	2.7768	0.0507	1.0904	3.7595	0.1522	1.0904	3.2777
Activity (µmol/mg-hr)			25.416			22.961			13.008	
Mean			2.077			2.883			3.114	
Standard Deviation			0.499			0.593			1.067	
CV (%)			24.021			20.583			34.267	

* EB = Enzyme Blank, SB = Substrate Blank, ES = Enzyme-Substrate Complex

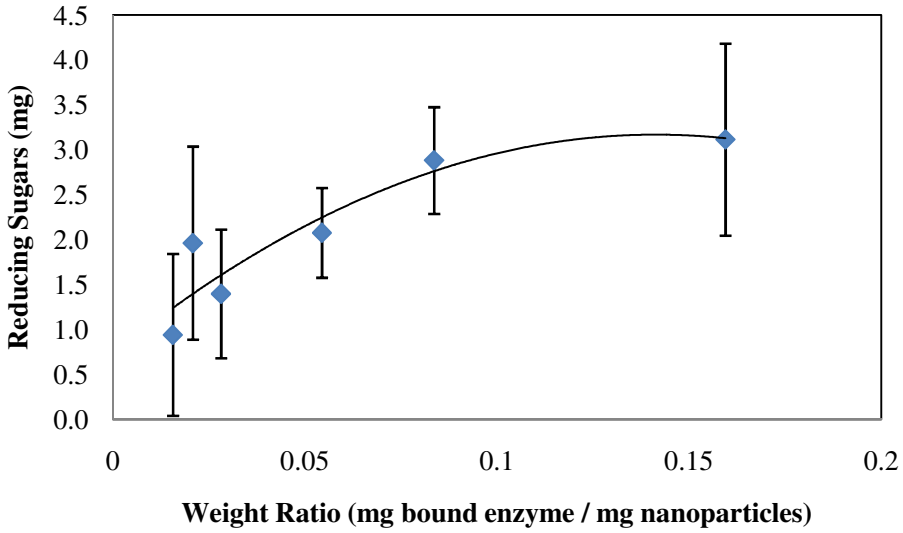

Figure B.2: Reducing sugar production over varying weight ratios.

Table B.3: Effect of temperature on reducing sugar production by free enzyme and statistical analysis.

Temperature (˚C)		25			30			40			50		
		EB	SB	ES	EB	SB	ES	EB	SB	ES	EB	SB	ES
Reducing	Replicate 1	0.07	2.308	2.587	0.038	2.447	3.519	0.032	2.549	5.148	0	2.498	5.744
Sugars	Replicate 2	0.025	2.251	2.929	0.013	2.473	3.474	0.051	2.91	5.173	0.025	2.181	5.287
(mg)	Replicate 3	0.057	2.447	2.859	0.063	2.308	3.747	0.051	2.587	5.319	0.025	1.566	5.547
Activity (µmol/mg-hr)		9.474			26.447			58.075			80.032		
Mean		0.406			1.133			2.487			3.428		
Standard Deviation		0.209			0.173			0.219			0.526		
CV (%)		51.389			15.270			8.816			15.359		

Temperature (˚C)		60			70			80		
		EB	SB	ES	EB	SB	ES	EB	SB	ES
Reducing	Replicate 1	0	1.75	5.135	0.025	2.58	4.894	0.101	2.143	2.878
Sugars	Replicate 2	0	1.953	4.736	0.082	2.606	4.539	0.108	1.636	2.79
(mg)	Replicate 3	0	1.839	4.527	0.044	2.618	4.634	0.184	2.111	2.847
Activity (µmol/mg-hr)		68.930			47.565			17.368		
Mean		2.952			2.037			0.744		
Standard Deviation		0.326			0.187			0.291		
CV (%)		11.026			9.183			39.158		

* EB = Enzyme Blank, SB = Substrate Blank, ES = Enzyme-Substrate Complex

Table B.4: Effect of temperature on reducing sugar production by immobilized enzyme and statistical analysis.

Temperature (˚C)		25			30			40			50		
		EB	SB	ES	EB	SB	ES	EB	SB	ES	EB	SB	ES
Reducing	Replicate 1	0.146	1.319	1.49	0.114	0.691	1.667	0.133	0.615	2.124	0.127	1.965	3.068
Sugars	Replicate 2	0.171	1.128	1.471	0.152	0.735	1.693	0.139	0.685	2.232	0.139	1.084	3.113
(mg)	Replicate 3	0.178	1.135	1.75	0.19	0.754	1.148	0.19	0.881	1.953	0.152	1.128	2.986
Activity (µmol/mg-hr)		4.922			14.519			28.447			35.485		
Mean		0.211			0.623			1.221			1.524		
SD		0.190			0.312			0.200			0.501		
CV (%)		90.083			50.010			16.339			32.867		

Temperature (˚C)		60			70			80		
		EB	SB	ES	EB	SB	ES	EB	SB	ES
Reducing	Replicate 1	0.108	0.837	2.314	0.101	0.894	2.079	0.146	0.983	1.439
Sugars	Replicate 2	0.114	0.875	2.498	0.076	0.919	2.029	0.165	1.097	1.528
(mg)	Replicate 3	0.101	0.989	2.631	0.127	0.875	1.953	0.146	0.78	1.42
Activity (µmol/mg-hr)		34.304			23.821			8.318		
Mean		1.473			1.023			0.357		
Standard Deviation		0.178			0.072			0.171		
CV (%)		12.077			7.058			47.852		

* EB = Enzyme Blank, SB = Substrate Blank, ES = Enzyme-Substrate Complex

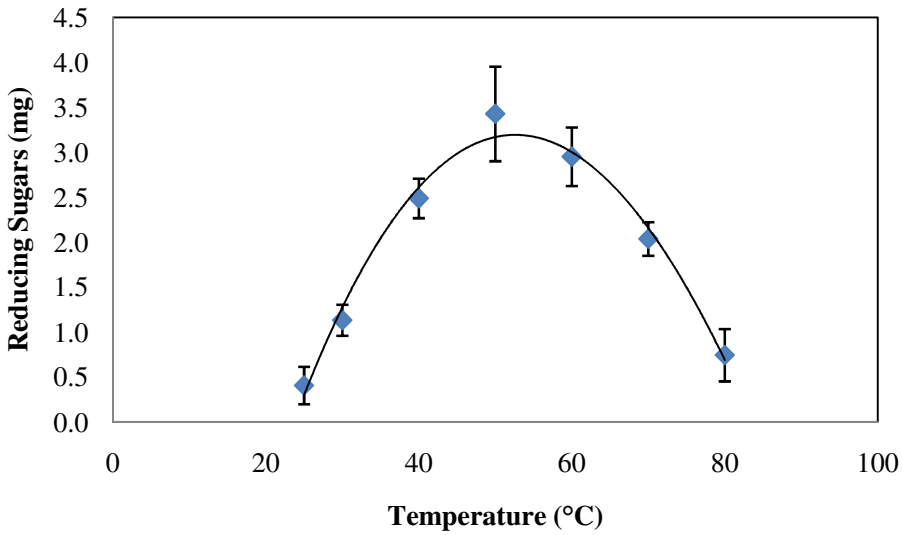

Figure B.3: Temperature profile for free cellulase enzyme.

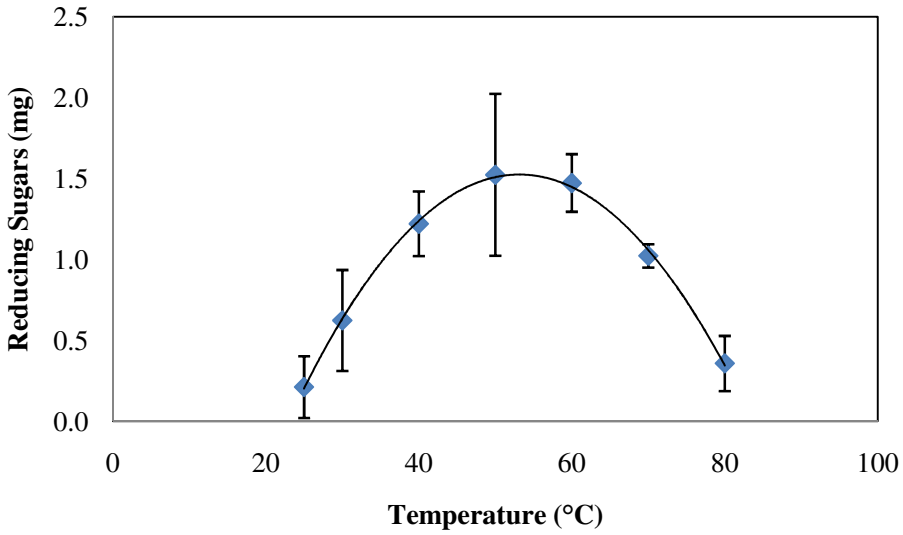

Figure B.4: Temperature profile for immobilized cellulase.

Table B.5: Effect of pH on reducing sugar production by free enzyme and statistical analysis.

pH		3			4			5			6			7		
		EB	SB	ES	EB	SB	ES	EB	SB	ES	EB	SB	ES	EB	SB	ES
Reducing Sugars (mg)	Replicate 1	0.04	2.43	3.4	0.1	2.24	4.98	0.15	2.07	4.43	0.01	2.31	3.46	0.05	1.79	2.14
	Replicate 2	0.04	2.41	3.38	0.11	1.97	4.38	0.14	2.3	4.63	0.03	1.83	3.41	0.06	1.9	2.47
	Replicate 3	0.06	2.4	3.09	0.12	2.31	4.34	0.16	2.16	4.34	0.04	2.32	3.57	0.06	2.1	2
Activity (µmol/mg-hr)		19.757			54.293			50.925			30.967			5.077		
Mean		0.831			2.282			2.141			1.302			0.213		
Standard Deviation		0.177			0.399			0.185			0.290			0.287		
CV (%)		21.315			17.466			8.653			22.298			134.486		

* EB = Enzyme Blank, SB = Substrate Blank, ES = Enzyme-Substrate Complex

Table B.6: Effect of pH on reducing sugar production by immobilized enzyme and statistical analysis.

pH		3			4			5			6			7		
		EB	SB	ES	EB	SB	ES	EB	SB	ES	EB	SB	ES	EB	SB	ES
Reducing Sugars (mg)	Replicate 1	0.06	0.86	1.33	0.05	0.55	1.86	0.13	1.31	3.35	0.1	0.79	1.86	0.08	0.72	0.82
	Replicate 2	0.09	0.84	1.41	0.08	0.58	1.95	0.13	1.08	2.9	0.11	0.56	1.88	0.13	0.71	0.67
	Replicate 3	0.1	0.68	1.31	0.12	0.59	2.1	0.13	1.13	3.07	0.11	0.68	1.91	0.18	0.86	0.81
Activity (µmol/mg-hr)		10.383			33.195			42.342			24.423			0.000		
Mean		0.478			1.317			1.803			1.099			0.000		
Standard Deviation		0.113			0.128			0.253			0.117			0.127		
CV (%)		23.647			9.754			14.047			10.664			0.000		

* EB = Enzyme Blank, SB = Substrate Blank, ES = Enzyme-Substrate Complex

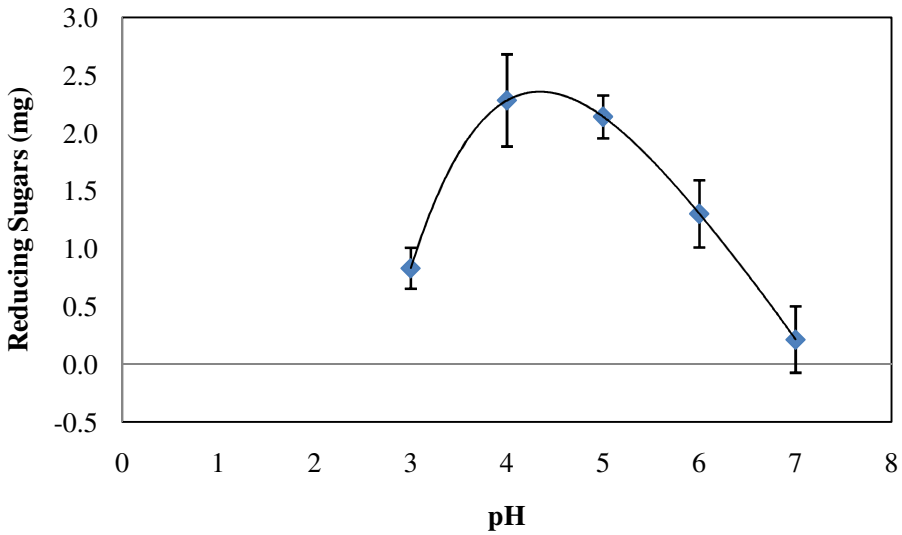

Figure B.5: pH profile for free cellulase enzyme.

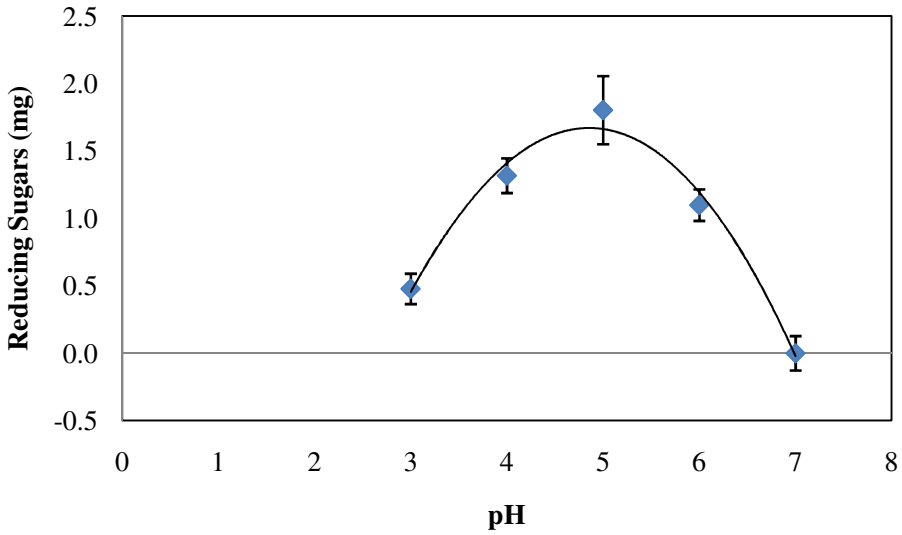

Figure B.6: pH profile for immobilized cellulase.

Table B.7: Reducing sugar production over time by free cellulase enzyme for determination of enzymatic stability.

Time (hours)		12			24			48			72		
		EB	SB	ES	EB	SB	ES	EB	SB	ES	EB	SB	ES
Reducing Sugars (mg)	Replicate 1	0.083	0	1.977	0.064	0.006	4.792	0.057	0.038	6.833	0.051	0	8.422
	Replicate 2	0.076	0	2.581	0.025	0.006	3.508	0.038	0.032	6.979	0.019	0.006	8.517
	Replicate 3	0.083	0	2.396	0.057	0.006	3.623	0.064	0.013	7.538	0.07	0.019	8.307
Activity (µmol/mg-hr)		3.348			2.811			2.523			1.998		
Mean		2.237			3.919			7.036			8.360		
Standard Deviation		0.309			0.711			0.373			0.109		
CV (%)		13.832			18.136			5.299			1.298		

* EB = Enzyme Blank, SB = Substrate Blank, ES = Enzyme-Substrate Complex

Table B.8: Reducing sugar production over time by cellulase-bound nanoparticles for determination of enzymatic stability.

Time (hours)		24			48			72			96		
		EB	SB	ES	EB	SB	ES	EB	SB	ES	EB	SB	ES
Reducing Sugars (mg)	Replicate 1	0.102	0.006	1.138	0.07	0	1.322	0.133	0.013	1.595	0.013	0	1.595
	Replicate 2	0.108	0.044	0.896	0.114	0.013	1.309	0.159	0.044	1.97	0.019	0	2.021
	Replicate 3	0.14	0.064	0.909	0.127	0.038	1.589	0.14	0.07	1.703	0.013	0	1.633
Activity (µmol/mg-hr)		0.599			0.488			0.381			0.286		
Mean		0.826			1.286			1.570			1.735		
Standard Deviation		0.141			0.162			0.196			0.236		
CV (%)		17.004			12.591			12.459			13.581		

* EB = Enzyme Blank, SB = Substrate Blank, ES = Enzyme-Substrate Complex

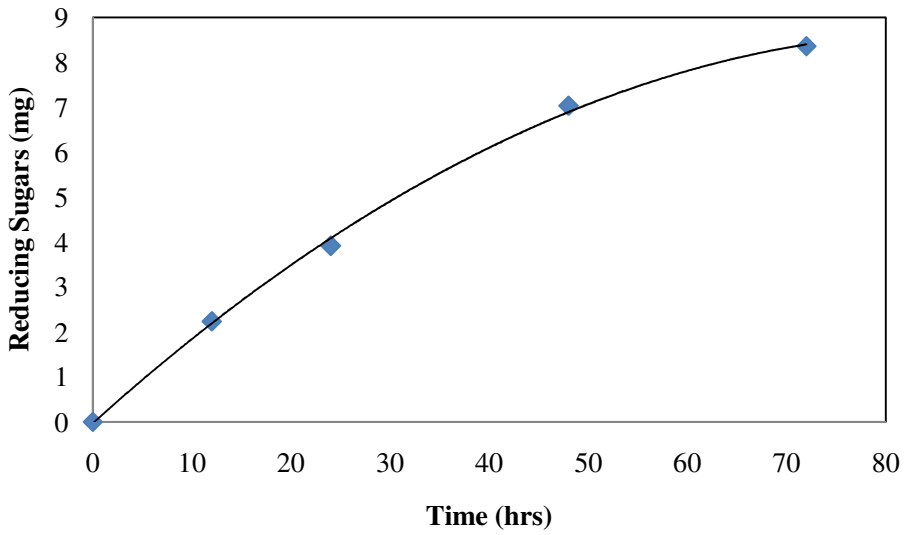

Figure B.7: Enzymatic stability for free cellulase enzyme during hydrolysis of cellulose.

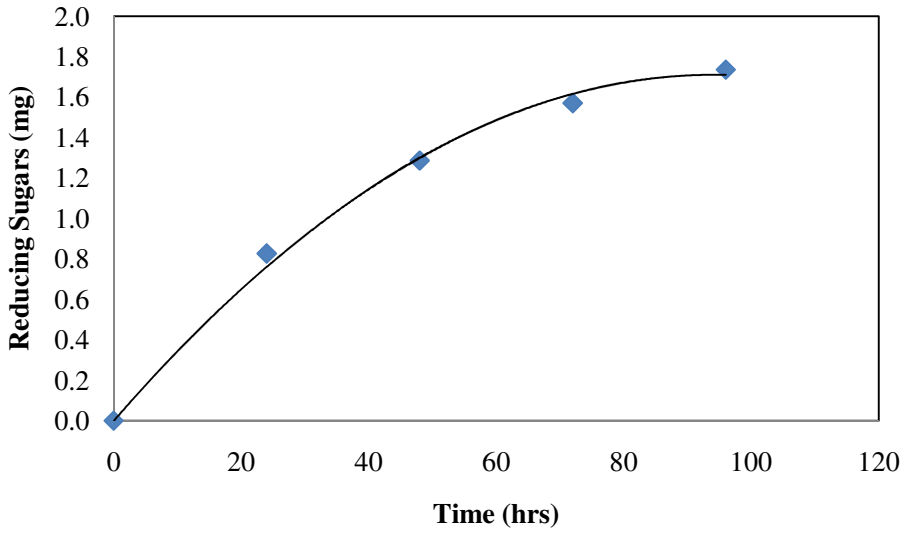

Figure B.8: Enzymatic stability for immobilized cellulase during hydrolysis of cellulose.

APPENDIX C: RAW DATA AND STATISTICS FOR RECYCLING OF POLYSTYRENE-COATED MAGNETIC MICROPARTICLES

Table C.1: Reducing sugars produced (mg) over 6 recycles of cellulase-bound, polystyrene-coated particles (1-2 μm).

	Time (hr)	24			48			72			96		
Recycle #	**Replicate #**	EB	SB	ES	EB	SB	ES	EB	SB	ES	EB	SB	ES
	1	0	0	8.13	0.08	0	18.6	0.48	0	27.1	0.4	0	33.2
0	2	0	0	8.37	0.4	0.08	18.5	0.56	0.08	23.9	1.27	0.16	29.2
	3	0	1.75	8.45	0.24	1.12	19.4	0.52	0.08	28.8	0.84	0	30.3
	1	0.16	0	4.54	1.27	0	7.01	1.12	0	11.6	1.27	0	10.2
1	2	0.4	0	4.14	1.83	0.4	8.92	1.27	0.32	8.61	1.51	0.4	14
	3	0.28	0	3.03	1.55	0.24	6.37	1.2	0	7.57	1.39	0.08	10.4
	1	0.96	0.32	2.23	0.8	0	2.87	0.48	0	4.06	0.8	0	5.42
2	2	0.72	0.4	2.23	0.96	0.4	3.67	1.12	0	4.78	0.88	0.4	5.26
	3	0.84	0	1.91	0.88	0	3.43	0.8	0.08	5.18	0.84	0	5.9
	1	0.08	0	0	0.48	0	1.04	0.48	0	2.23	0.88	0.64	3.35
3	2	0.08	0	0.4	0.32	0	1.35	0.56	0.48	2.63	1.04	0.8	3.11
	3	0.08	0	0.96	0.4	0	2.07	0.52	0	2.39	0.96	0	3.75
	1	1.04	0	1.2	0	0	0	1.59	0.24	2.31	0.96	0.56	2.31
4	2	0.96	0.08	1.12	0	0	0	0.96	0.8	3.03	1.35	0.56	3.03
	3	1	0	0.8	0	0.32	1.35	1.27	0	2.23	1.16	0.56	3.35

* EB = Enzyme Blank, SB = Substrate Blank, ES = Enzyme-Substrate Complex

Table C.2: Statistical analysis for reducing sugars produced by recycled polystyrene-coated particles.

Recycle #	Statistic	Time (hr)			
		24	48	72	96
0	Mean	7.729	18.194	26.042	30.027
	SD	1.026	0.794	2.505	2.115
	CV (%)	13.269	4.365	9.620	7.044
1	Mean	3.625	5.671	7.942	9.973
	SD	0.794	1.371	2.077	2.177
	CV (%)	21.895	24.172	26.151	21.830
2	Mean	1.049	2.311	3.851	4.555
	SD	0.304	0.476	0.651	0.406
	CV (%)	29.004	20.594	16.893	8.905
3	Mean	0.372	1.089	1.740	1.965
	SD	0.480	0.536	0.343	0.536
	CV (%)	129.165	49.266	19.744	27.296
4	Mean	0.013	0.345	0.903	1.182
	SD	0.219	0.803	0.679	0.567
	CV (%)	1652.271	232.684	75.216	47.947

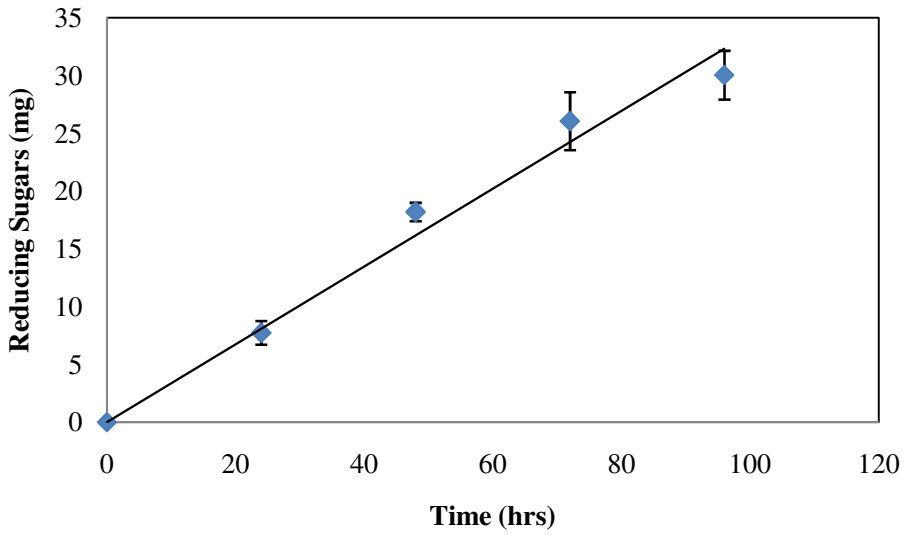

Figure C.1: Mean reducing sugar production for initial hydrolysis of enzyme-bound polystyrene-coated particles.

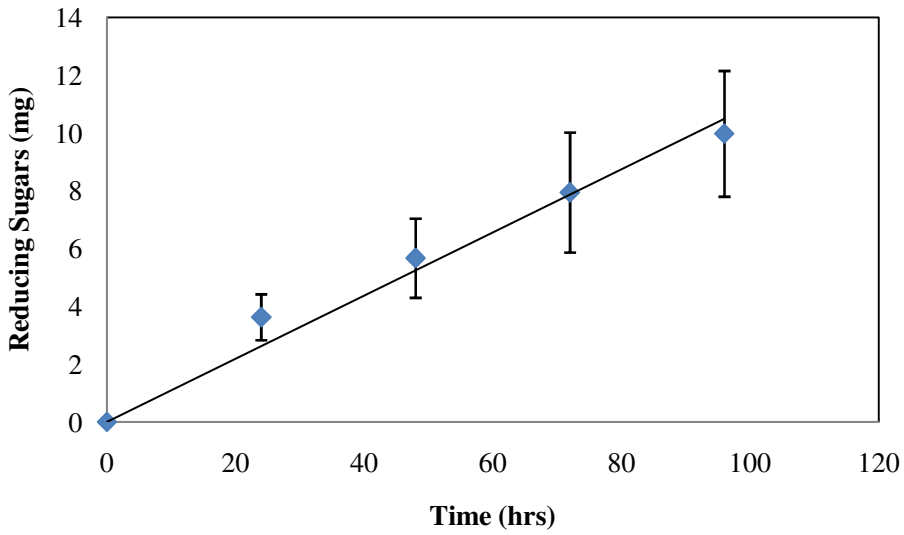

Figure C.2: Mean reducing sugar production for the 1st recycle of enzyme-bound polystyrene-coated particles.

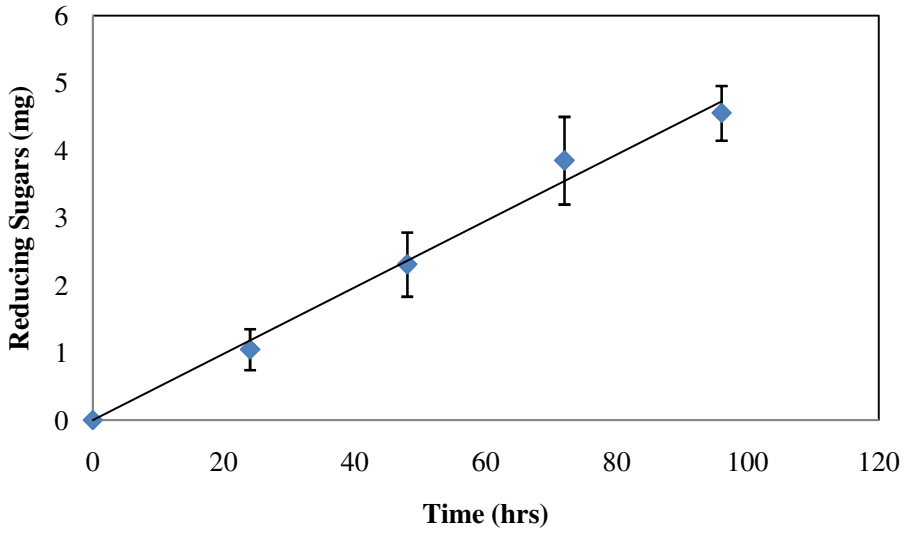

Figure C.3: Mean reducing sugar production for the 2nd recycle of enzyme-bound polystyrene-coated particles.

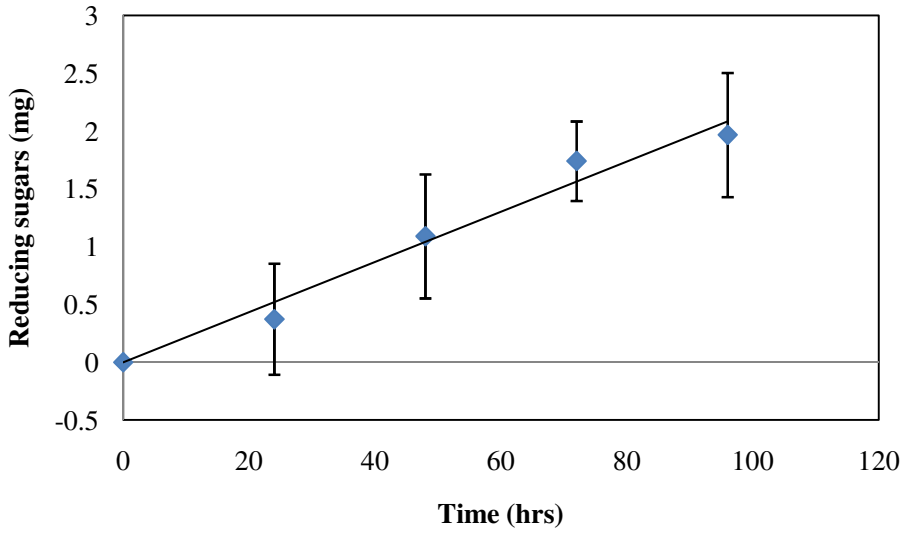

Figure C.4: Mean reducing sugar production for the 3rd recycle of enzyme-bound polystyrene-coated particles.

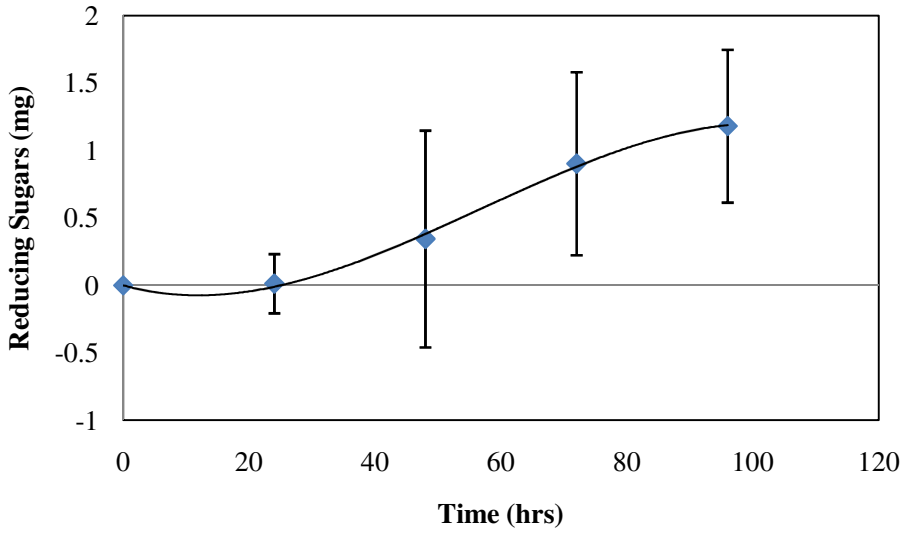

Figure C.5: Mean reducing sugar production for the 4th recycle of enzyme-bound polystyrene-coated particles.

VITA

Jason Jordan was born in December of 1981 in McComb, Mississippi. He grew up with his family in Vidalia, Louisiana, where he attended Vidalia High School. Upon graduation, he started his college career at Louisiana Tech University in Ruston, Louisiana, majoring in electrical engineering. He later transferred to Louisiana State University in Baton Rouge, Louisiana where he graduated in 2006 with a Bachelor of Science in Biological and Agricultural Engineering. After a short stint as a field engineer in the oil services industry, he returned to LSU to pursue his Master of Science in Biological and Agricultural Engineering degree, which will be awarded in August 2009. His technical interests include bioprocessing and alternative energy sources.